OAK RIDGE NATIONAL LABORATORY LIBRARIES
3 4456 0570509 2

K/CSD/TM-56

MARTIN MARIETTA

COMPUTING AND TELECOMMUNICATIONS DIVISION

ANALYSIS OF CALIBRATED HOT BOX DATA FOR THREE CONCRETE WALLS

K. W. Childs

OPERATED BY
MARTIN MARIETTA ENERGY SYSTEMS, INC.
FOR THE UNITED STATES
DEPARTMENT OF ENERGY

DISCLAIMER

This report was prepared as an account of work sponsored by an agency of the United States Government. Neither the United States Government nor any agency thereof, nor any of their employees, makes any warranty, express or implied, or assumes any legal liability or responsibility for the accuracy, completeness, or usefulness of any information, apparatus, product, or process disclosed, or represents that its use would not infringe privately owned rights. Reference herein to any specific commercial product, process, or service by trade name, trademark, manufacturer, or otherwise, does not necessarily constitute or imply its endorsement, recommendation, or favoring by the United States Government or any agency thereof. The views and opinions of authors expressed herein do not necessarily state or reflect those of the United States Government or any agency thereof.

K/CSD/TM-56
Dist. Category UC 95c

ANALYSIS OF CALIBRATED HOT BOX DATA FOR THREE CONCRETE WALLS

K. W. Childs
Technical Applications

Date Issued: September 1985

COMPUTING AND TELECOMMUNICATIONS DIVISION
at
Oak Ridge Gaseous Diffusion Plant
Post Office Box P
Oak Ridge, Tennessee 37831

Martin Marietta Energy Systems, Inc.
operating the
Oak Ridge Gaseous Diffusion Plant
Oak Ridge Y-12 Plant
Oak Ridge National Laboratory
Paducah Gaseous Diffusion Plant
under contract No. DE-AC05-84OR21400
for the
Department of Energy

Table of Contents

List of Figures vii

Abstract 1

1. Introduction 1

2. Test Facility 1

3. Test Walls and Cycles 4

4. Comparison of Calculated and Experimental Results 4

5. Influence of Errors in Surface Temperature Measurements 7

6. Influence of Wall Surface Temperature on Flow Patterns 24

7. Influence of the Mass of the Calibrated Hot Box 39

8. Influence of Uncertainty in Wall Properties 41

9. Conclusions and Recommendations 42

Acknowledgments 45

References 47

List of Figures

Figure		Page
1.	Schematic of calibrated hot box	2
2.	Outdoor temperature cycles	6
3.	Heat flux at the inside surface of wall C1 - NBS - 10°F cycle	8
4.	Heat flux at the inside surface of wall C1 - NBS + 10°F cycle	9
5.	Heat flux at the inside surface of wall C2 - NBS - 10°F cycle	10
6.	Heat flux at the inside surface of wall C2 - NBS + 10°F cycle	11
7.	Heat flux at the inside surface of wall C3 - NBS - 10°F cycle	12
8.	Heat flux at the inside surface of wall C3 - NBS + 10°F cycle	13
9.	Heat flux at the inside surface of wall C1 - step change in outdoor air temperature	14
10.	Heat flux at inside surface of wall C1 - numerical experiment with an error in the inside surface temperature	18
11.	Heat flux at inside surface of wall C1 - numerical experiment with an error in the outside surface temperature	19
12.	Heat flux at inside surface of wall C1 - numerical experiment with errors in inside and outside surface temperature	20
13.	Heat flux at inside surface of wall C3 - numerical experiment with an error in the inside surface temperature	21
14.	Heat flux at inside surface of wall C3 - numerical experiment with an error in the outside surface temperature	22
15.	Heat flux at inside surface of wall C3 - numerical experiment with errors in inside and outside surface temperature	23

List of Figures (cont.)

Figure		Page
16.	Streamlines in outdoor flow channel - isothermal case	25
17.	Velocity profile in outdoor flow channel 7.25 feet from the entrance	26
18.	Streamlines in outdoor flow channel - hot wall case	28
19.	Velocity Profile in outdoor flow channel 7.25 feet from the entrance - hot wall case	29
20.	Isotherms in outdoor flow channel - hot wall case	30
21.	Streamlines in outdoor flow channel - cold wall case	31
22.	Velocity profile in outdoor flow channel 7.25 feet from the entrance - cold wall case	32
23.	Isotherms in outdoor flow channel - cold wall case	33
24.	Heat Flux at outside surface of wall C1 versus surface/air temperature difference	34
25.	Heat flux at outside surface of wall C1 versus surface/air temperature difference - NBS cycle + 10°F	36
26.	Heat flux at outside surface of wall C1 versus surface/air temperature difference - NBS cycle	37
27.	Heat flux at outside surface of wall C1 versus surface/air temperature difference - NBS cycle - 10°F	38
28.	Influence of hot box mass on observed lag in heat flux at inside surface of test wall	40

ANALYSIS OF CALIBRATED HOT BOX DATA FOR THREE CONCRETE WALLS

K. W. Childs

ABSTRACT

Three walls constructed of concrete with different densities were tested in a calibrated hot box at the Construction Technology Laboratories of the Portland Cement Association. The observed dynamic performance of these walls was not in good agreement with analytical solutions based on the assumption of linear heat conduction through the walls. Several sources of potential errors in the data from the hot box were explored. While some of these errors do appear to be real, they do not fully explain the discrepancy between experimental and analytical results. The experimentally determined values of the specific heats for the three concrete walls were identified as the most likely cause for the discrepancies. This report presents the analysis of the data from the hot box experiments and suggestions for future investigation.

1. INTRODUCTION

In recent years the calibrated hot box has been introduced as a tool in the evaluation of the thermal performance of building envelope systems under both steady-state and dynamic conditions. The results of tests run under carefully controlled conditions, along with analytical and field studies, can lead to a better understanding of the behavior of building thermal envelopes and ultimately improved design criteria. Specifically, the calibrated hot box offers the opportunity to evaluate the accuracy of analytical methods currently being used. The objective of this report is to make a comparison between experimental results from a calibrated hot box and analytical solutions for three specific walls and, to the extent possible, explain the cause of any discrepancies.

2. TEST FACILITY

The data used in this study are from a calibrated hot box facility owned and operated by Construction Technology Laboratories of Skokie, Illinois, which is a division of the Portland Cement Association. The brief description of the facility included in this section should give the reader sufficient understanding of its operation to follow the analysis. A more complete description is presented in Ref. 1.

A schematic of the calibrated hot box is shown in Fig. 1. The facility consists of (from left to right in the figure) an outdoor environmental chamber, a frame which holds the wall to be tested, and an indoor environmental chamber. Both of the environmental chambers and the test frame are highly insulated to minimize heat flow between the hot box and its surroundings. Overall dimensions of the test wall are 103 x 103 inches (262 x 262 cm). Both the indoor and outdoor chambers have internal dimensions of 103 x 103 x 41 inches (262 x 262 x 104 cm). A baffle in each environmental chamber defines an air flow channel next to the test wall. In each of the environmental chambers the baffle is 6.5 inches (16.5 cm) from the end nearest the test wall, but the flow channel widths may be greater than this if the test wall is thinner than its frame.

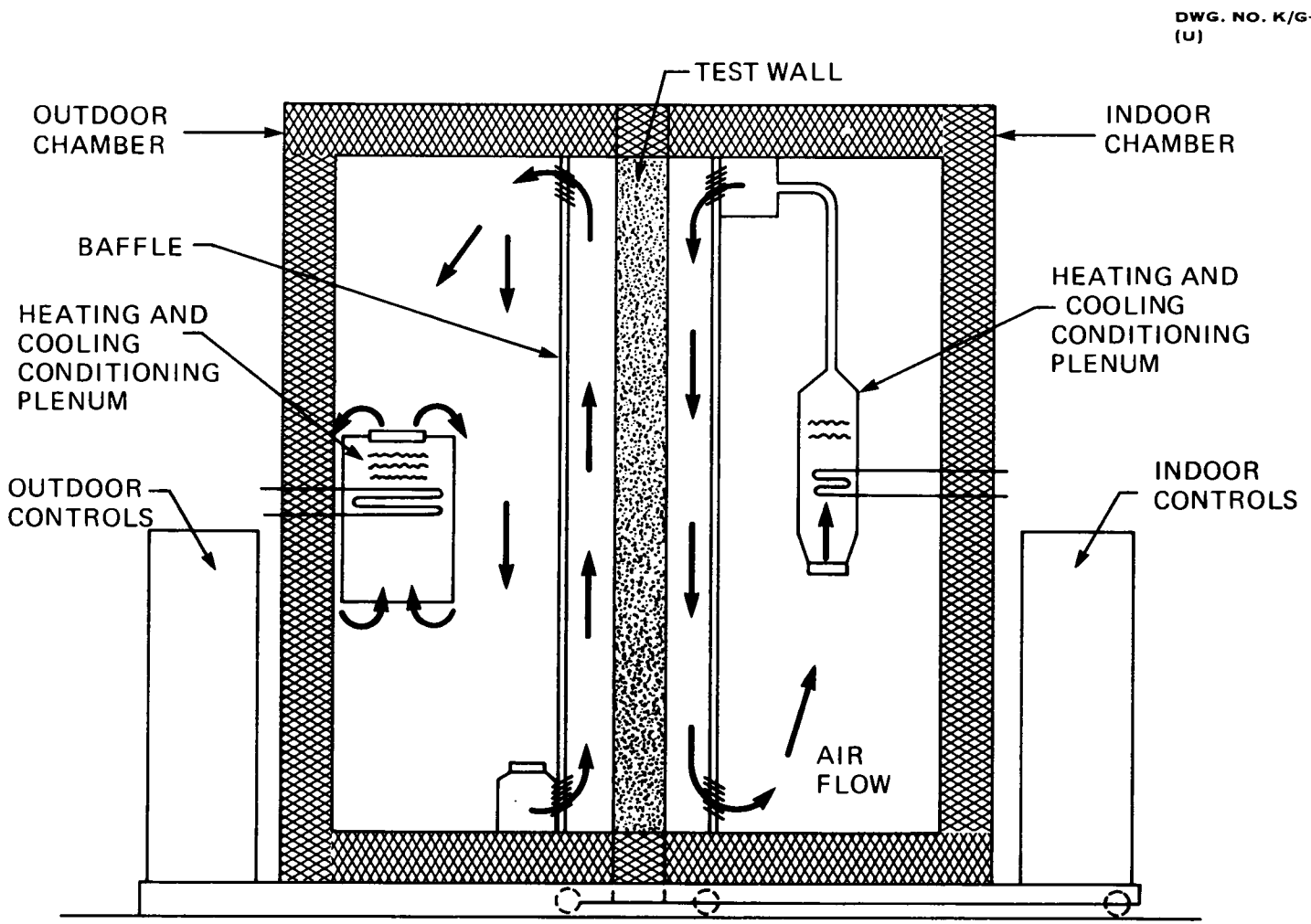

Fig. 1. Schematic of calibrated hot box.

The outdoor chamber heating and cooling equipment can be programmed such that the air temperature in the chamber follows any desired time-temperature relationship. The range of temperature is from -15 to 130°F (-26 to 54°C). There is a 1000 cfm (0.47 m^3/s) mixing fan to ensure that the air temperature is uniform throughout the outdoor chamber and a 280 ft^3/min ($0.13 m^3/s$) circulating fan to move air in an upward direction through the channel adjacent to the test wall. Based on the rated air flow for the fan, the mean air velocity in the channel is at most 1 ft/s (0.3 m/s). It will be less if the distance from the test wall surface to the baffle defining the air flow channel is greater than 6.5 inches (16.5 cm).

In the indoor chamber, air is drawn into a heating and cooling plenum by a 280 cfm (0.13 m^3/s) circulating fan. The plenum is connected by means of a supply duct to the channel adjacent to the test wall where the air flow is in a downward direction. Heat is added to or removed from the plenum as necessary to maintain a constant air temperature at the entrance to the flow channel. The indoor chamber temperature can be maintained at any value between 65 and 80°F (18 and 27°C). In the indoor chamber the maximum mean air velocity in the flow channel is 1 ft/s (0.3 m/s).

The overall instrumentation of the calibrated hot box is documented in Ref. 1 and will not be discussed in any detail. Only the data of particular relevance to the current discussion will be addressed. These are:

1. the average air temperature in the flow channels on either side of the test wall (the average of 16 values arranged on a 4 x 4 grid approximately 3 inches (7.6 cm) from the wall in each channel),

2. the average surface temperature on both sides of the test wall (the average of 16 values on each surface),

3. the surface heat flux on both sides of the test wall (determined by heat flux transducers mounted on each surface), and

4. the heat flux at the surface of the wall adjacent to the indoor chamber (determined by measuring the net energy input or removed at the indoor heating and cooling conditioning plenum).

There is heat transfer to or from the indoor chamber other than that coming through the test wall. This introduces an error in the heat flux determined by measuring the energy added to or removed from the indoor chamber conditioning plenum. The two main sources of this error are heat transfer between the indoor chamber and the laboratory and heat transfer between the indoor and outdoor chambers through the box structure rather than through the test wall. The measured heat flux is corrected for these known sources of error. To obtain this correction the hot box is "calibrated" with a test wall made of a homogeneous material of known properties. The procedure used in this calibration is described in Ref. 1. The corrected value for heat flux is considered to be more accurate than the heat flux transducer and is the value used in most of the analyses to be presented.

3. TEST WALLS AND CYCLES

There were three concrete walls tested differing primarily in the type of concrete used in their construction. These walls are designated C1, C2, and C3 in order of decreasing density. Wall C1 is a normal weight concrete wall. The mixture consists of Portland cement, Elgin sand and gravel, and Vinsol resin air-entraining admixture. There is a single layer of reinforcement near the midplane of the wall consisting of grade 60 number 5 bars spaced 12 inches (30.5 cm) on centers. At the time of testing, the wall had a unit weight of 100 lb/ft^2 (488 kg/m^2), an average thickness of 8.31 inches (21.1 cm), a surface area of 73.5 ft^2 (6.84 m^2), and an estimated moisture content of 2.1% based on ovendry weight.

Wall C2 is a structural lightweight concrete wall. The mixture consists of Portland cement, expanded shale aggregate, and Vinsol resin air-entraining admixture. There is a single layer of reinforcement near the midplane of the wall consisting of grade 60 number 5 bars spaced 12 inches (30.5 cm) on centers. At the time of testing, the wall had a unit weight of 70.4 lb/ft^2 (344 kg/m^2), an average thickness of 8.28 inches (21.0 cm), a surface area of 73.67 ft^2 (6.84 m^2), and an estimated moisture content of 8.5% based on ovendry weight.

Wall C3 is a low density concrete wall. The mixture consists of Portland cement, perlite aggregate, and Vinsol resin air-entraining admixture. There is a single layer of reinforcement near the midplane of the wall consisting of 0.24 inch (6 mm) bars spaced 12 inches (30.5 cm) on centers. At the time of testing, the wall had a unit weight of 32.7 lb/ft^2 (160 kg/m^2), an average thickness of 8.52 inches (21.6 cm), a surface area of 73.79 ft^2 (6.86 m^2), and an estimated moisture content of 9.5% based on ovendry weight. Material properties for all three of the walls are given in Table 1. The values are from Refs. 2, 3, and 4 for walls C1, C2, and C3, respectively.

The primary outdoor temperature cycle used in testing the walls is what is commonly referred to as the National Bureau of Standards (NBS) cycle.[5] This cycle was used by NBS in an early experimental study of building energy use. While this is not an accepted "standard" cycle, it has been widely used in both experimental and analytical studies. The NBS cycle is shown in Fig. 2 along with two additional cycles derived by shifting the temperature 10°F (5.6°C) above or below the NBS cycle. In addition to the NBS cycles, some data are presented for a step change in the outdoor air temperature. For all of the tests the indoor air temperature was held constant.

4. COMPARISON OF CALCULATED AND EXPERIMENTAL RESULTS

In order to make a comparison between experimental results obtained from dynamic tests in the calibrated hot box and analytical results, the data from seven tests[2,3,4] were examined. These tests include two dynamic tests for each of the three walls and a step temperature change transient for the normal weight concrete wall. The two dynamic cycles used for each of the walls are the NBS cycle minus 10°F and the NBS cycle plus 10°F. Since this is a check between hot box results and analytical results, the conductivities used in all of the calculations were obtained from steady-state hot box runs. The film resistances on the inside and outside surfaces of the test wall were also obtained from steady-state runs of the hot box. However, since these values show unexplained variations from run to run and from wall to wall, average values were used in all of the calculations. One possible reason for some of this variation is addressed in a subsequent section. The average values used for film resistances are 0.268 hr-ft^2-°F/Btu (0.0472 m^2-K/W) for the inside and 0.400 hr-ft^2-°F/Btu (0.0705 m^2-K/W) for the outside.

Table 1. Material properties for the concretes in this study.

	Wall					
	C1		C2		C3	
Density - lb/ft^3 (kg/m^3)	144.0	(2310.0)	102.0	(1630.0)	46.0	(740.0)
Specific Heat - Btu/lbm°F (J/kg-K)	0.185	(745.0)	0.181	(758.0)	0.163	(682.0)
Thermal Conductivity Btu/hr-ft-°F (W/m-K)						
Hot Box	0.975	(1.69)	0.394	(0.681)	0.120	(0.208)
Hot Wire - Air Dry	1.69	(2.89)	0.500	(0.865)	0.254	(0.439)
Hot Wire - Oven Dry	1.13	(1.95)	0.350	(0.605)	0.124	(0.214)
Hot Plate - Oven Dry	1.34	(2.32)	0.375	(0.649)	0.120	(0.208)

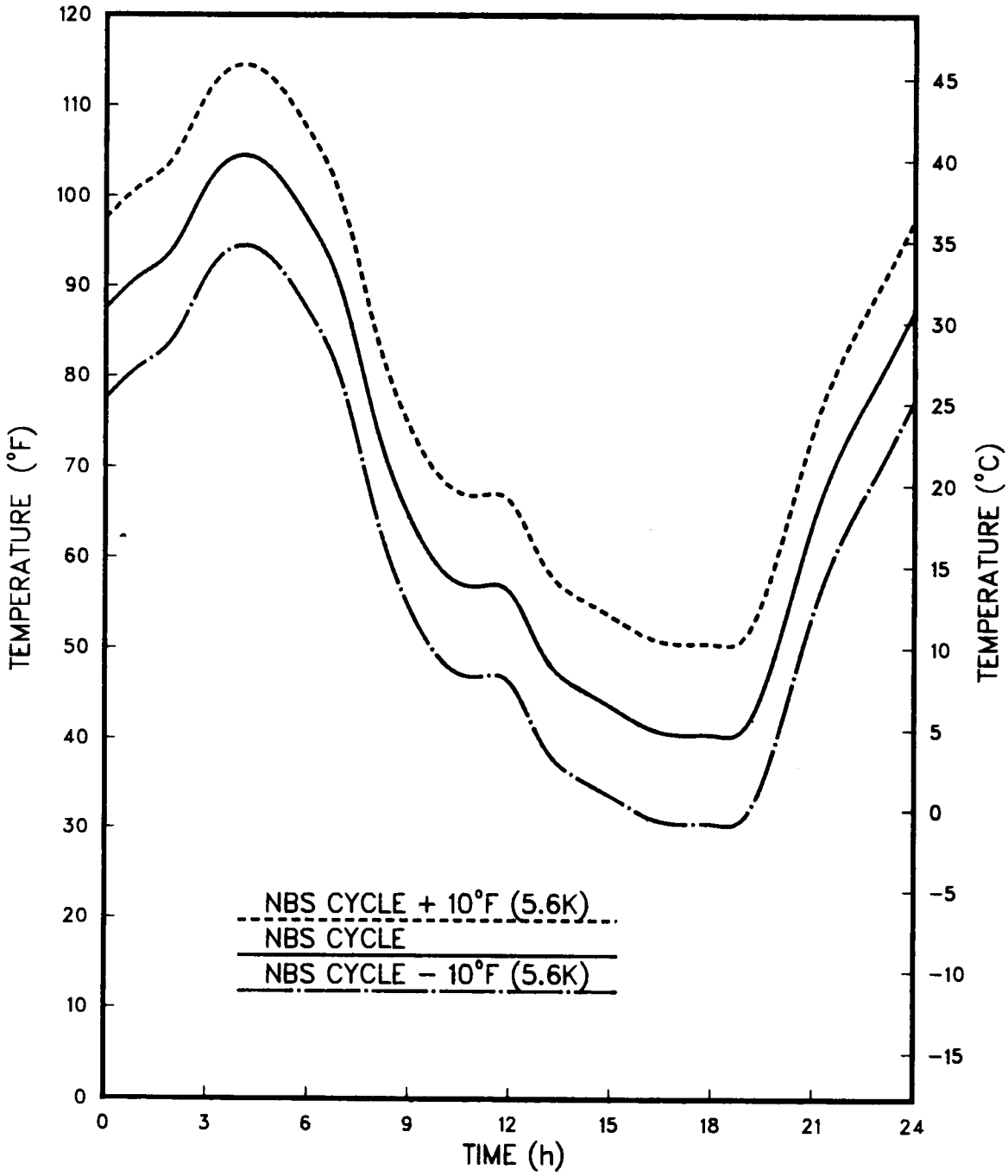

Fig. 2. Outdoor temperature cycles.

The analytical solutions were developed using a computer program written specifically to do these analyses. The calculational technique is basically the National Bureau of Standards response factor method.[6] The results from one test case were verified by using a finite difference heat transfer computer program, HEATING6.[7] The heat flux at the inside surface of the test wall is used for the comparison of experimental versus calculated results. The heat flux at the inside surface was calculated two ways: (1) using the measured air temperatures and response factors calculated from one air stream to the other, and (2) using the measured surface temperatures and the response factors calculated from one wall surface to the other. Figure 3 presents the results of the calculations for the normal weight concrete wall subjected to the NBS cycle minus 10°F. The time in this figure is not the time of day but the time into the 24 hour cycle relative to an arbitrary reference time.

The heat flux obtained from the repeated application of a steady-state heat transfer equation at each hour of the 24 hour cycle is plotted in the figure. This provides a convenient reference for judging time lags and amplitude reductions in the heat flux at the inside surface since the steady-state results contain no lag or amplitude reduction. Also shown on the plot are the measured heat flux and the two heat fluxes determined from the response factor calculations. Figures 4 through 8 are similar plots for the other cycles and walls. Figure 9 is a plot of these heat fluxes versus time for a step change in the air temperature in the outdoor chamber while the indoor chamber air temperature is maintained constant. As can be seen by the steady-state heat transfer plots, a hot box can not truly obtain a step temperature change.

Several observations can be made about the results presented in the figures of this section. First, both a time lag and an amplitude reduction in the heat flux at the inside surface of the wall are quite evident in the measured and calculated values for all of the tests. Second, and more important from the standpoint of this investigation, there is not very good agreement between the measured heat flux and the values calculated using either of the response factor methods. In all cases the response factor calculations predict both a smaller time lag and amplitude reduction than was experimentally observed. Third, the two alternate ways of calculating heat fluxes using response factors produce different results. While this difference is not particularily dramatic, it is consistently present throughout all of the cases and is an indication of a problem. Fourth, although there is not good hour-to-hour agreement between calculated and measured heat fluxes, there is good agreement in the average heat flux over an entire period (i.e., in each of Figs. 3 through 8, all four of the heat flux curves presented have approximately the same 24 hour average). In the case involving a step change in the outdoor air temperature, there is a significant difference between each of the response factor calculations and the measured heat fluxes during the transient portion, yet they all converge to the same steady-state value. In the following sections possible reasons for these observed discrepancies are discussed.

5. INFLUENCE OF ERRORS IN SURFACE TEMPERATURE MEASUREMENTS

It was assumed in all of the analyses performed in this study that the conductivity of the wall and film coefficients were constants (i.e., they were not temperature dependent). In this case, for a steady periodic test the average heat flux over one cycle is dependent only on the overall R value of the wall and the average temperature difference across the wall. This allows a check on the R value independent of the wall density or specific heat. The fact that the calculated average heat flux and the measured heat flux are in good agreement would seem to indicate that the R values for the wall and air films are correct. However, that conclusion may not be justified. The fact that there is a difference between the heat flux calculated from one air stream to the other and the heat flux calculated from one wall surface to the other is particularly troublesome. If the R values for the wall and the air streams are indeed correct, these two calculations should produce the same results since the other wall parameters (density, specific heat, and thickness) are the same in both calculations. The fact that the two calculated results are not the same casts doubt on the accuracy of these R values.

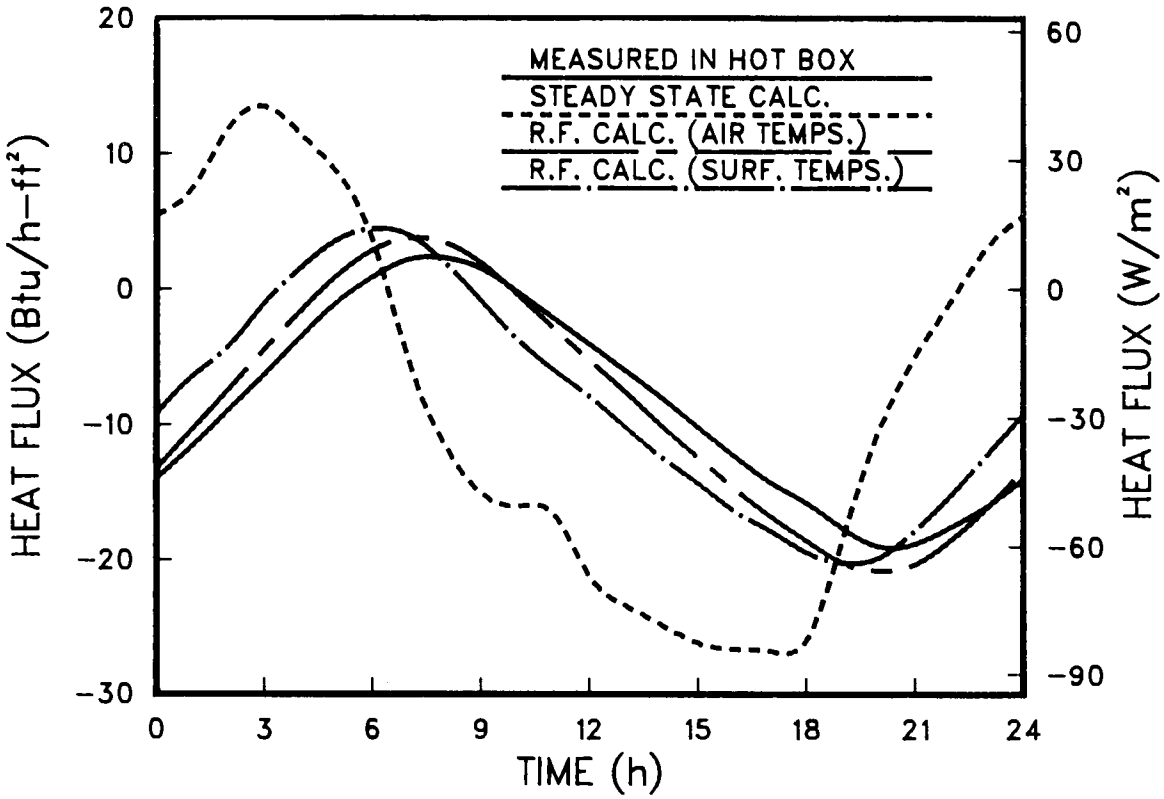

Fig. 3. Heat flux at the inside surface of wall C1 - NBS - 10°F cycle.

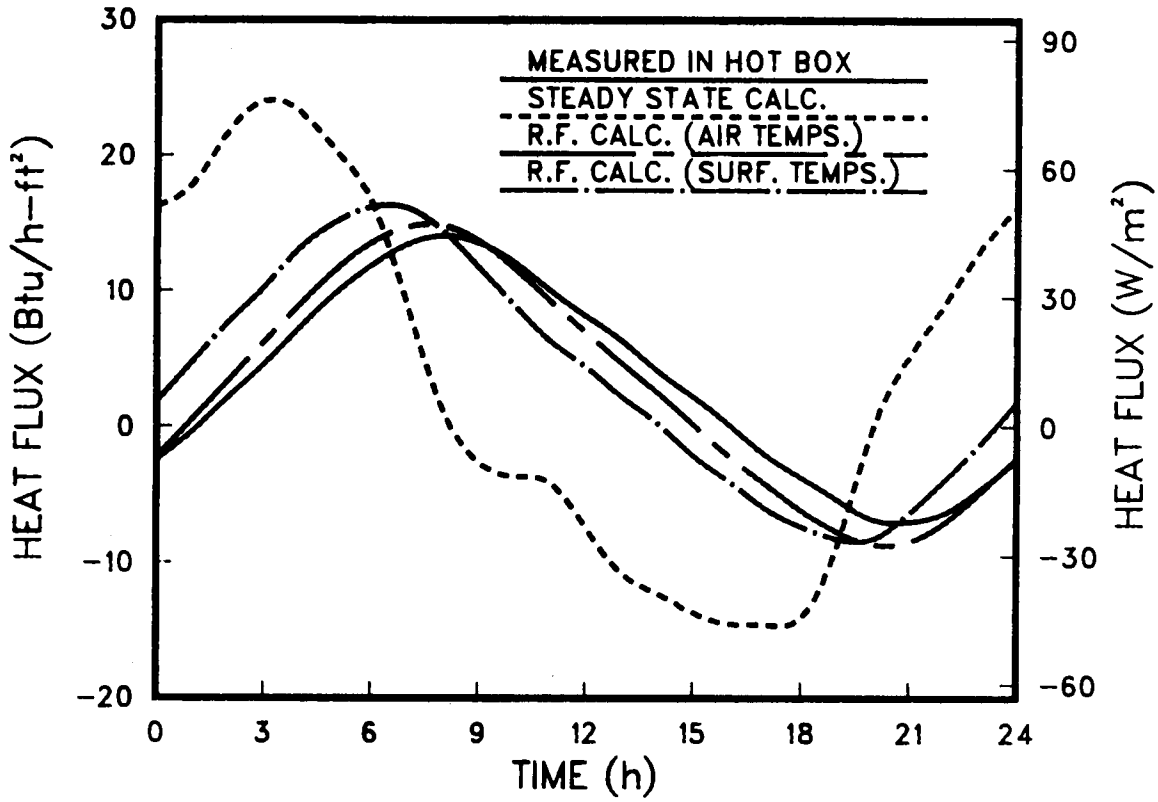

Fig. 4. Heat flux at the inside surface of wall C1 - NBS + 10°F cycle.

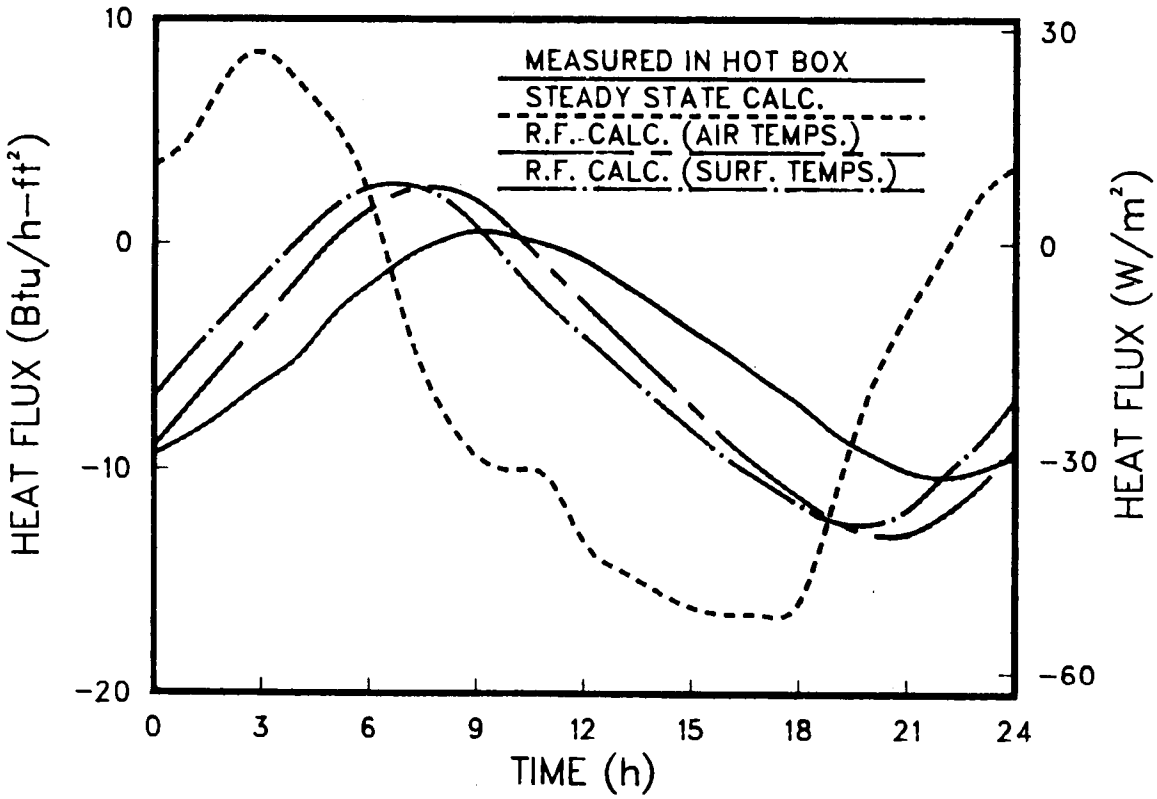

Fig. 5. Heat flux at the inside surface of wall C2 - NBS - 10°F cycle.

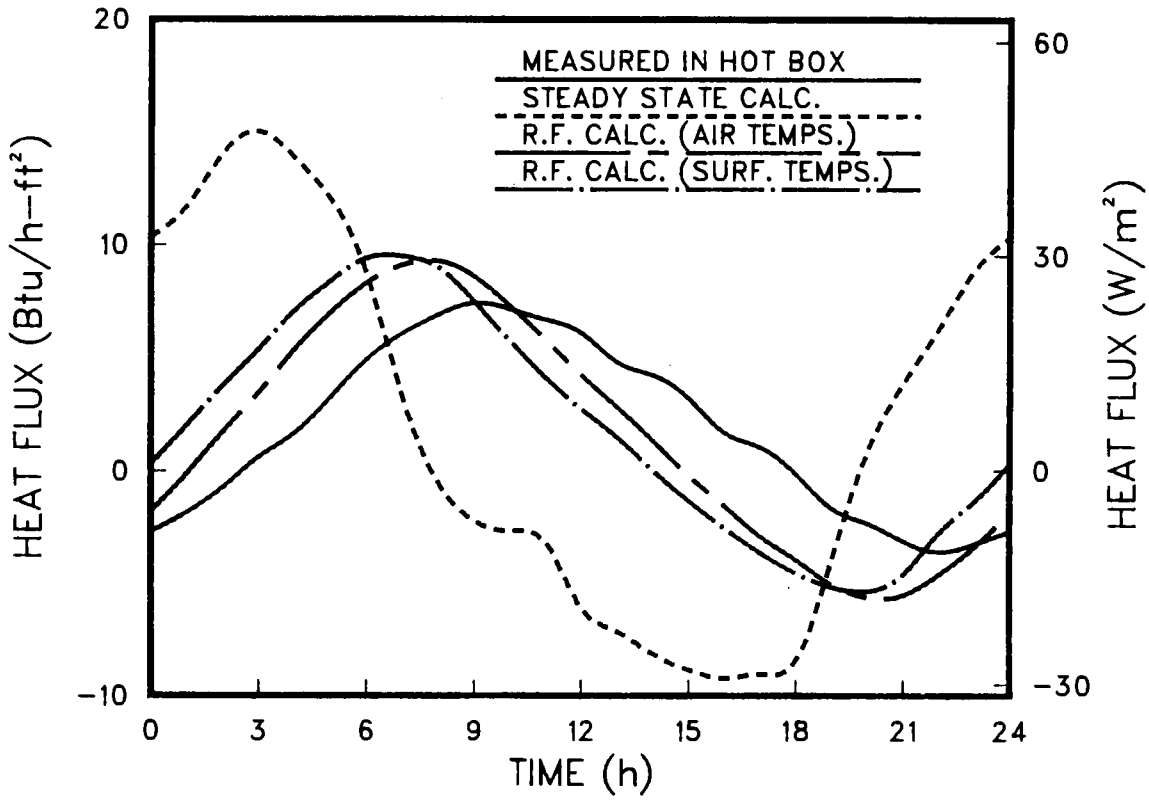

Fig. 6. Heat flux at the inside surface of wall C2 - NBS + 10°F cycle.

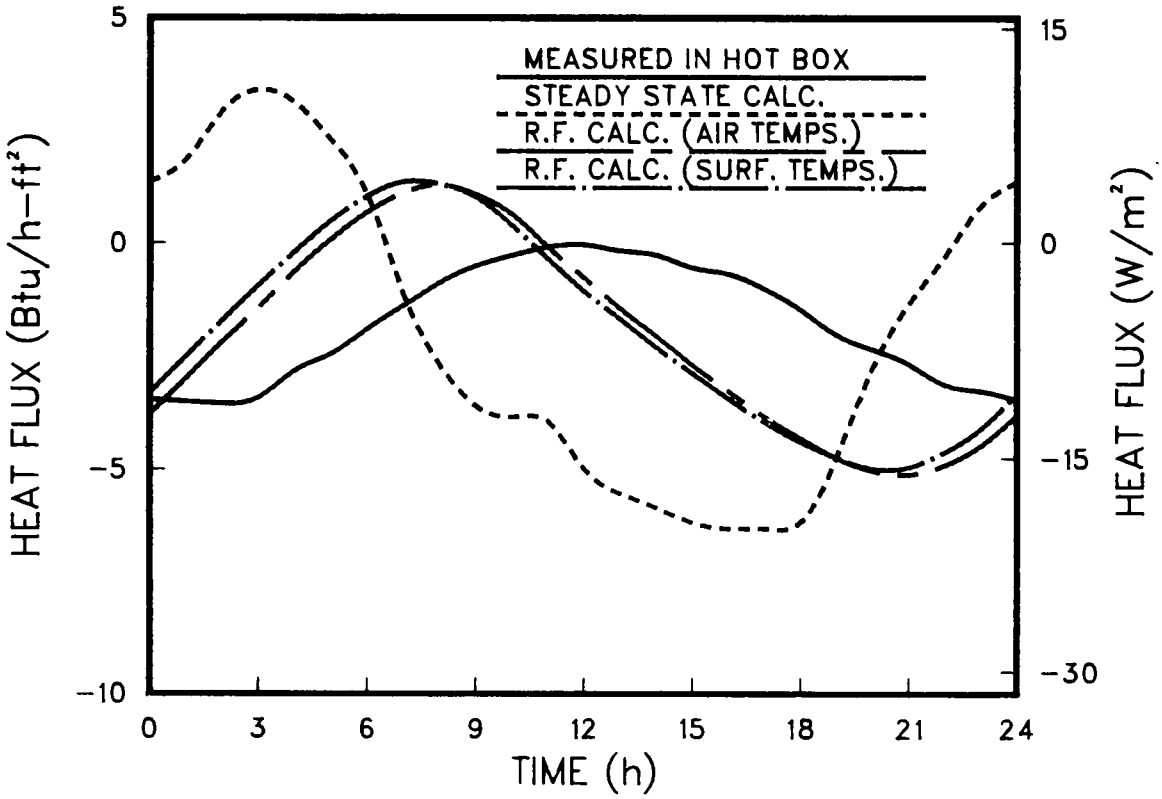

Fig. 7. Heat flux at the inside surface of wall C3 - NBS - 10°F cycle.

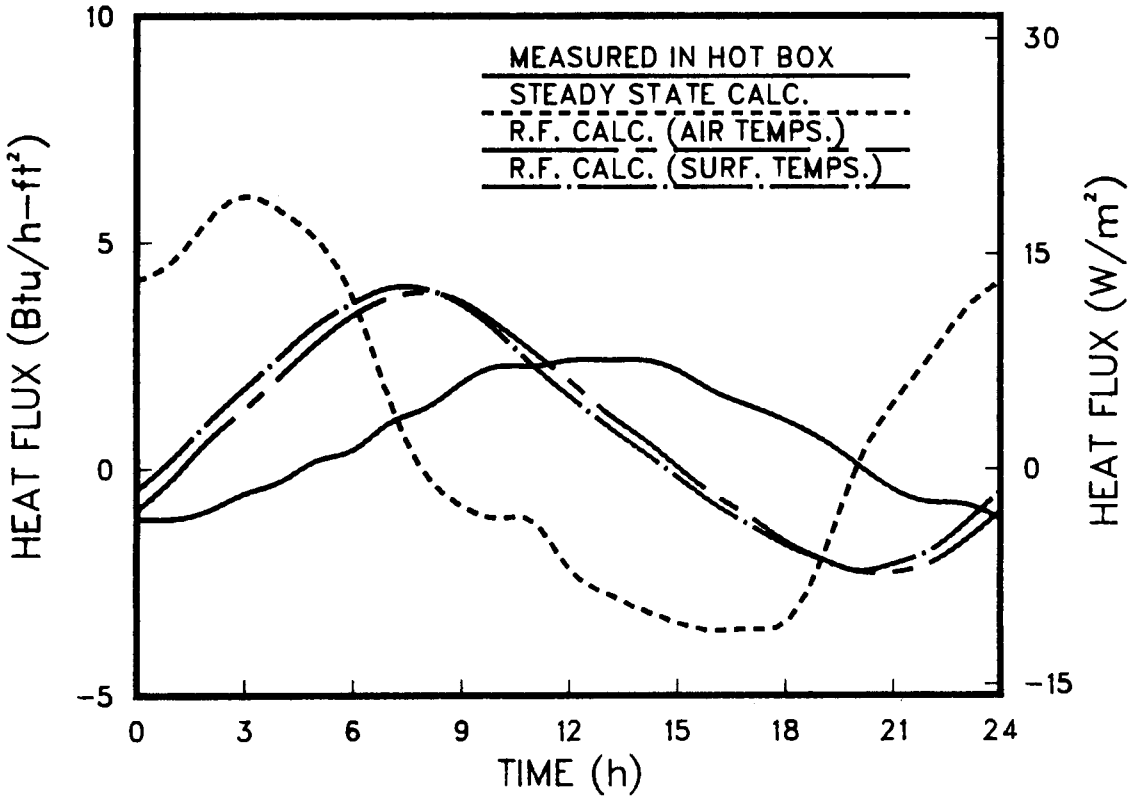

Fig. 8. Heat flux at the inside surface of wall C3 - NBS + 10°F cycle.

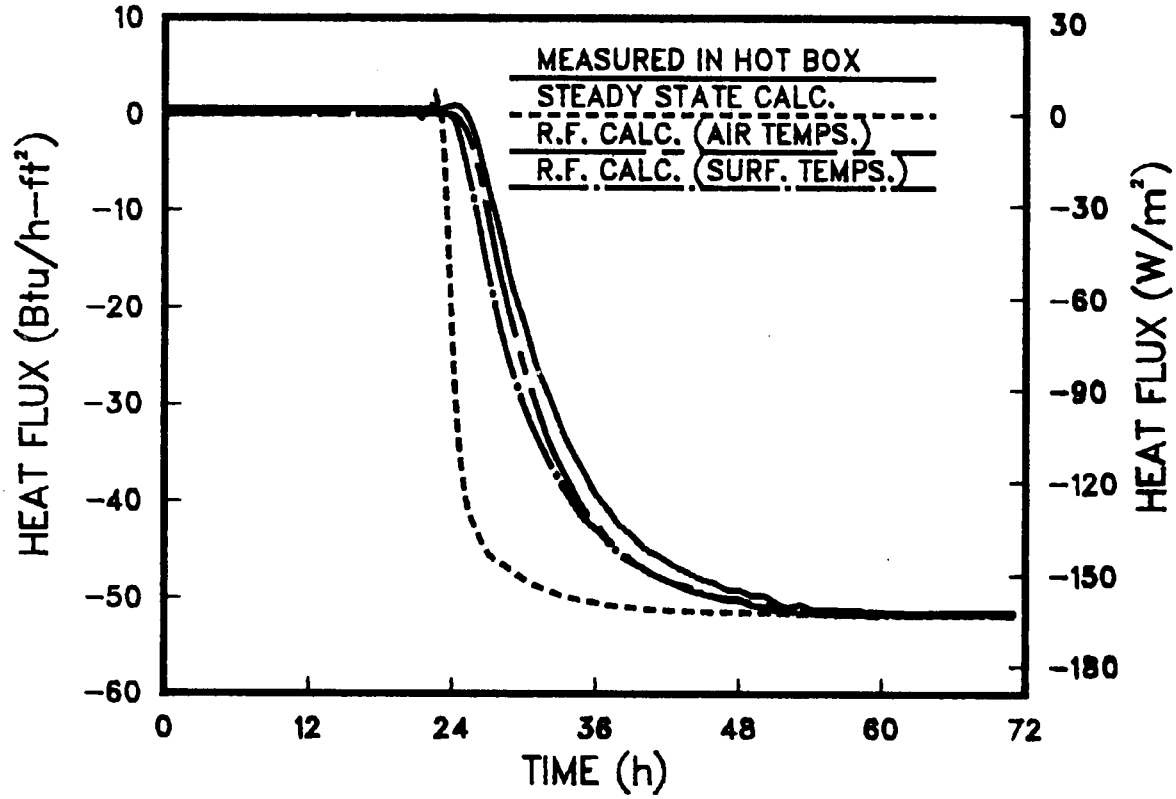

Fig. 9. Heat flux at the inside surface of wall C1 - step change in outdoor air temperature.

In trying to determine a possible cause for the discrepancy in the calculated fluxes, the experimental procedure and the data were scrutinized. In this process the measured surface temperatures were identified as being a possible source of error. Since the thermal conductivity and the film coefficients used were derived from steady-state experiments, an erroneous measurement of surface temperature would result in erroneous R values.

The first 3 inches (7.6 cm) of the thermocouple leads are taped to the wall using duct tape. The edges of the tape are secured to the wall with epoxy cement. The thermocouples leads are 20 gauge (0.035 inches/0.90 mm).

It is hypothesized that the thermocouple is not indicating the true surface temperature, but rather is indicating a temperature between the actual surface temperature and the surrounding air temperature. The thermocouple is not in perfect thermal contact with the surface nor is it thermally isolated from the surrounding air. The thermocouple may be acting somewhat as a fin, with heat being conducted along its leads and exchanged with the surrounding air. Thus, it seems reasonable to assume that the thermocouple will indicate a temperature between the surface and air temperature. In this situation, the R value for the wall determined from steady-state data will be too large and the R values for the surface film resistances will be too small. However, the total R value for the combined wall and film resistances will be correct. Thus the response factor calculation done from air to air will produce the correct value for the average heat flux for the 24 hour cycle, but the calculated hourly values for heat flux will not be correct.

For the response factor calculation done from surface to surface, it seems that errors in both the wall R value and surface temperature would result in an error in the calculated average heat flux. In a steady-state test, the contact resistance between the thermocouple junction and the surface and the effective thermal resistance between the thermocouple and the surrounding air determine the value for temperature that a surface mounted thermocouple will indicate. The indicated surface temperature is between the true surface temperature and the surrounding air temperature. This fractional position of the indicated temperature between the true surface and air temperatures is determined by the relative magnitude of the two resistances mentioned. These two resistances can probably be assumed constants (i.e., they will have the same values throughout the dynamic tests as they did in the steady-state tests). Thus the indicated surface temperature will be the same fraction of the way between the true surface temperature and the surrounding air temperature throughout the dynamic tests as it was in the steady-state tests. The measured surface temperatures in the dynamic test are in error in the same manner as those in the steady-state tests used to determine the R values. Even though both the surface temperature and wall R value are incorrect, they are consistent and will produce the correct average heat flux. This will not produce the correct dynamic performance.

If the preceding hypothesis is indeed true and there is a systematic error in the surface temperature measurement, it could possibly explain some of the observed discrepancies between different calculated results or between calculated and measured results. There is supporting evidence that the surface temperatures are in error. The wall thermal conductivities arrived at by material testing are higher than those determined from the hot box tests. This is consistent with the hypothesis.

In order to further test the hypothesis a "numerical experiment" was devised. In this numerical experiment the surface temperature and heat flux data were determined from a response factor calculation using the air stream temperatures as boundary conditions rather than from an actual hot box experiment. The data from this numerical experiment contained absolutely no experimental error. All thermal parameters needed for subsequent calculations were known exactly, an advantage which did not exist in the actual experiments. Specific errors were introduced in order to observe the effect they had on results. These effects were unobscured by experimental errors or other factors.

The wall conductivity used to generate the experimental data in the numerical experiment was determined using the hot wire method and is given in Table 1. The film resistances on the inside and outside were assumed to be equal. Their value was chosen so that the total R value (the test wall plus the two air films R values) matched the hot box experimental value. A response factor calculation was performed using an NBS cycle plus 10°F for the outdoor air temperature. The heat flux at the inside surface of the wall and the surface temperature on both surfaces were determined from this calculation. These are the "correct" values for heat flux and surface temperature. Three cases were generated in which there was an error introduced in one or both of the surface temperatures. All three cases were devised so that the apparent thermal conductivity of the wall from the numerical experiment would match the value from the actual hot box experiment. The three cases were generated as follows.

For Case 1, it was assumed that there was an error only in the measured indoor surface temperature. Thus, for the response factor calculation, the correct value for the outside air film R value was used. Erroneous values were used for the inside air film and the wall R values. The assumed erroneous wall R value was from the actual hot box tests (i.e. the same value used in the analysis of actual hot box data discussed in the previous section). The value used for the inside air film resistance was that which gave the correct overall R value. The erroneous values for the inside surface temperatures were obtained by moving the temperature a fraction of the way from the actual surface temperature to the air temperature. The value of this fraction was that which would have been necessary to produce the erroneous wall and air film R values used.

Case 1 results from the numerical experiment for the normal weight concrete wall are presented in Fig. 10 . These results are presented in a manner identical to those from the actual experiment in the previous section except that there are no errors in the data other than those intentionally introduced. Any discrepancies between calculated heat flux and the measured heat flux (labeled "actual heat flux" in the figure since there is no experimental error) are a result of an error in measuring the inside surface temperature. The two calculated heat flux curves differ from each other in both phase and amplitude. The heat flux determined using the surface temperatures has a longer lag time and smaller amplitude than the one using air temperatures. Neither calculated curve agrees with the actual heat flux. The heat flux calculated using air temperatures is approximately in phase with but has a larger amplitude than the actual heat flux. The heat flux calculated using the surface temperatures has approximately the same amplitude but a longer lag time than the actual heat flux.

Case 2 is very similar to Case 1 except that the error is assumed to be in the outside, rather than the inside, surface temperature. The results for this case are presented in Fig. 11. Once again there is no agreement among either of the two heat fluxes calculated with response factors or the actual heat flux. The behavior of the heat flux calculated using the air temperatures is the same as in Case 1. The calculated and actual heat fluxes are approximately in phase with each other but the amplitude of the calculated value is greater. For the heat fluxes calculated using the surface temperatures the behavior for Case 2 is reversed from that observed for Case 1. The amplitude of the calculated heat flux is greater than the actual heat flux and the lag time is less. The deviation from the actual heat flux in Case 2 is greater than in Case 1.

Case 3 is a combination of Cases 1 and 2. An error is assumed to occur in both the inside and outside surface temperatures. The error in each of the surface temperatures is half of the corresponding error in either Case 1 or 2. The results for this case are presented in Fig. 12. As anticipated, the results fall between Cases 1 and 2 but the behavior is more like Case 2. It appears that an error in measuring the outside surface temperature has a more significant impact on the calculated results than a similar error in the inside surface temperature.

A comparison of the results for the normal weight concrete wall from the numerical experiments with those from the actual experiments reveals some similarities in the behavior. The differences in behavior observed between the heat fluxes calculated using air and surface temperatures in the analysis of the actual data are very similar to those observed in the numerical experiments in which there was an error in the outside surface temperature. While this certainly does not constitute proof that there is an error in the measured surface temperatures, when considered along with the discrepancies in the measured conductivities, it does strongly suggest it. However, in the analysis of the actual experimental data, the measured heat flux lags behind the calculated values by a small but distinct time. This is not reflected in any of the results from the numerical experiment. Thus an error in the measured surface temperature does not explain this.

Another set of numerical experiments identical to those described above was performed for the lightweight insulating concrete wall. The results of the calculations using the data from these numerical experiments are presented in Figs. 13, 14, and 15. The observed effects produced by errors introduced in the inside and/or outside surface temperatures are qualitatively similar to those already presented but of smaller magnitude. However, this behavior is consistent with the results of calculations performed on the actual hot box data. The results from the numerical experiment do not reflect the observed large differences in lag time between the measured heat flux and the calculated values. The amount that the measured heat flux lags behind the calculated values is much greater for this wall than it was for the normal weight concrete wall. This indicates even more conclusively that there is a source of disagreement in the calculations beyond a surface temperature measurement error.

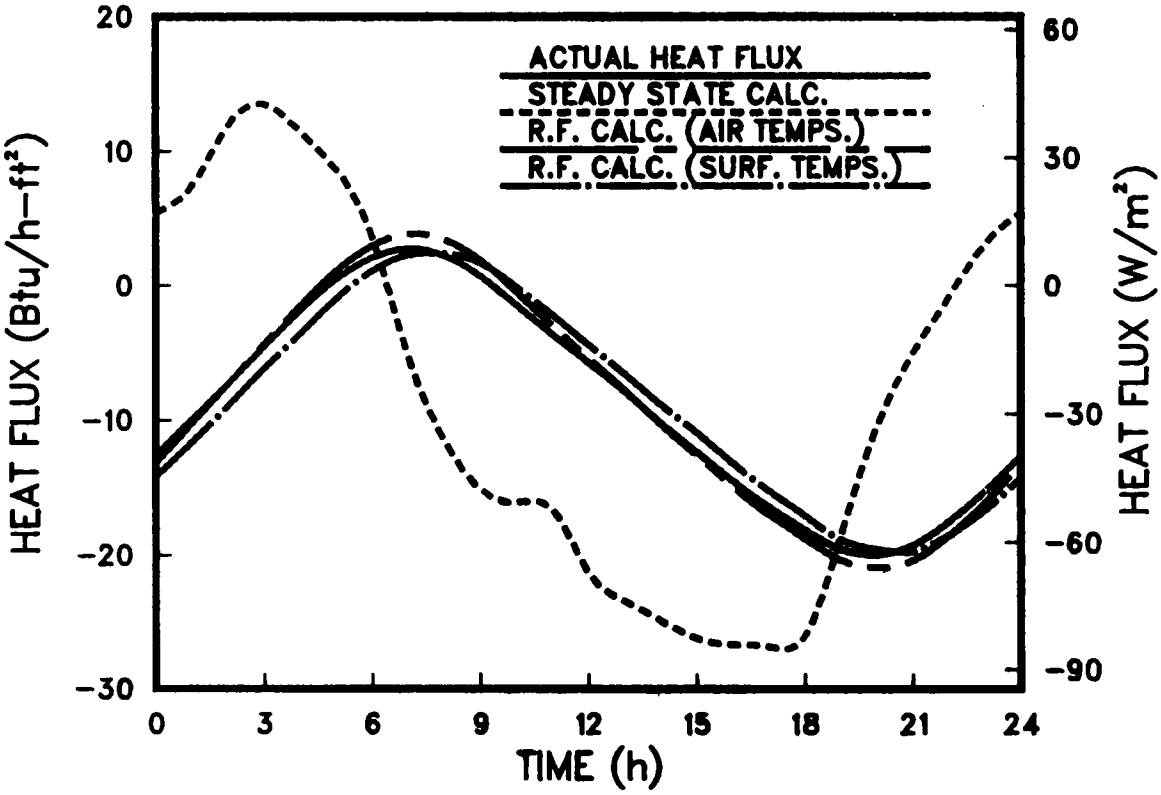

Fig. 10. Heat flux at inside surface of wall C1 - numerical experiment with an error in the inside surface temperature.

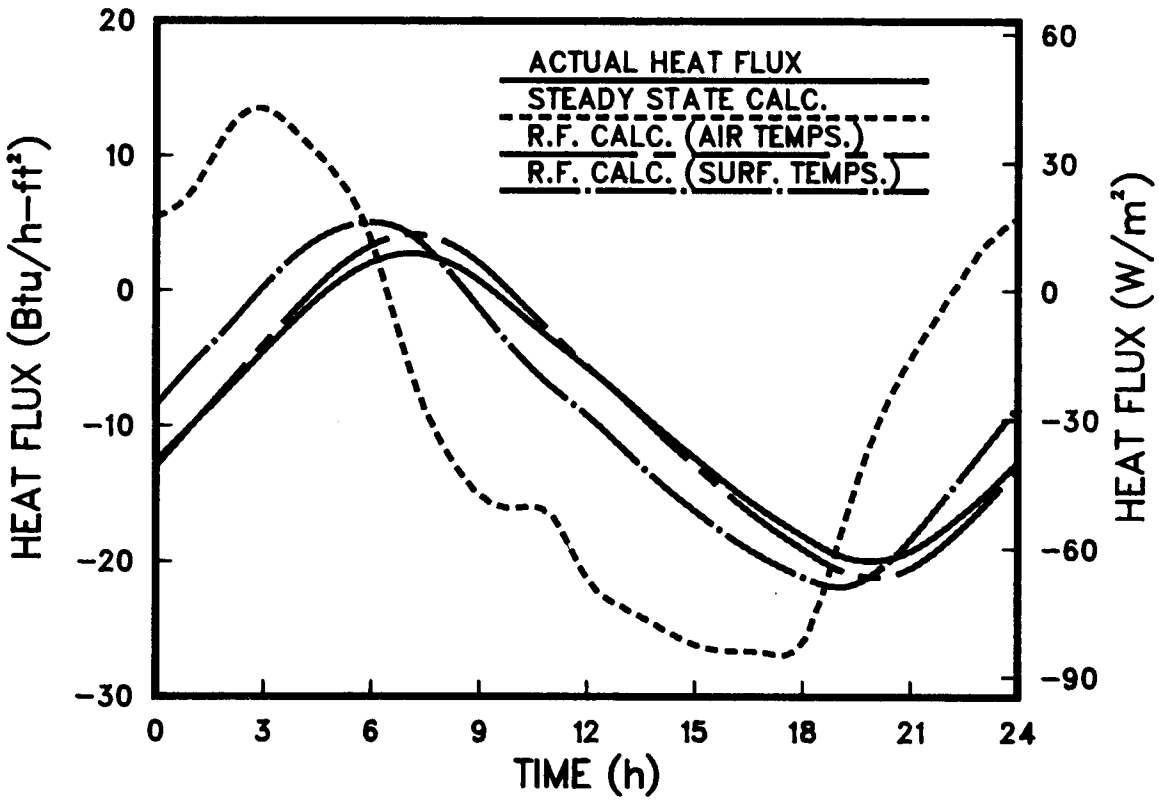

Fig. 11. Heat flux at inside surface of wall C1 - numerical experiment with an error in the outside surface temperature.

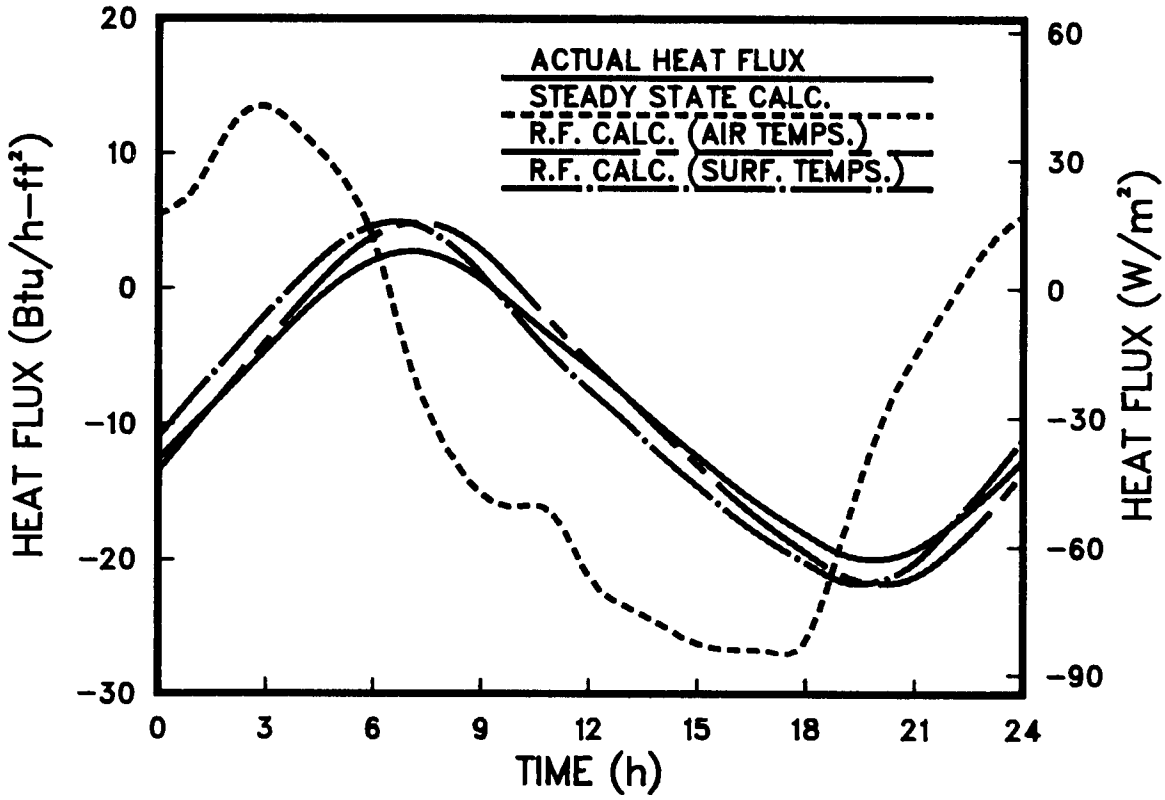

Fig. 12. Heat flux at inside surface of wall C1 - numerical experiment with errors in inside and outside surface temperature.

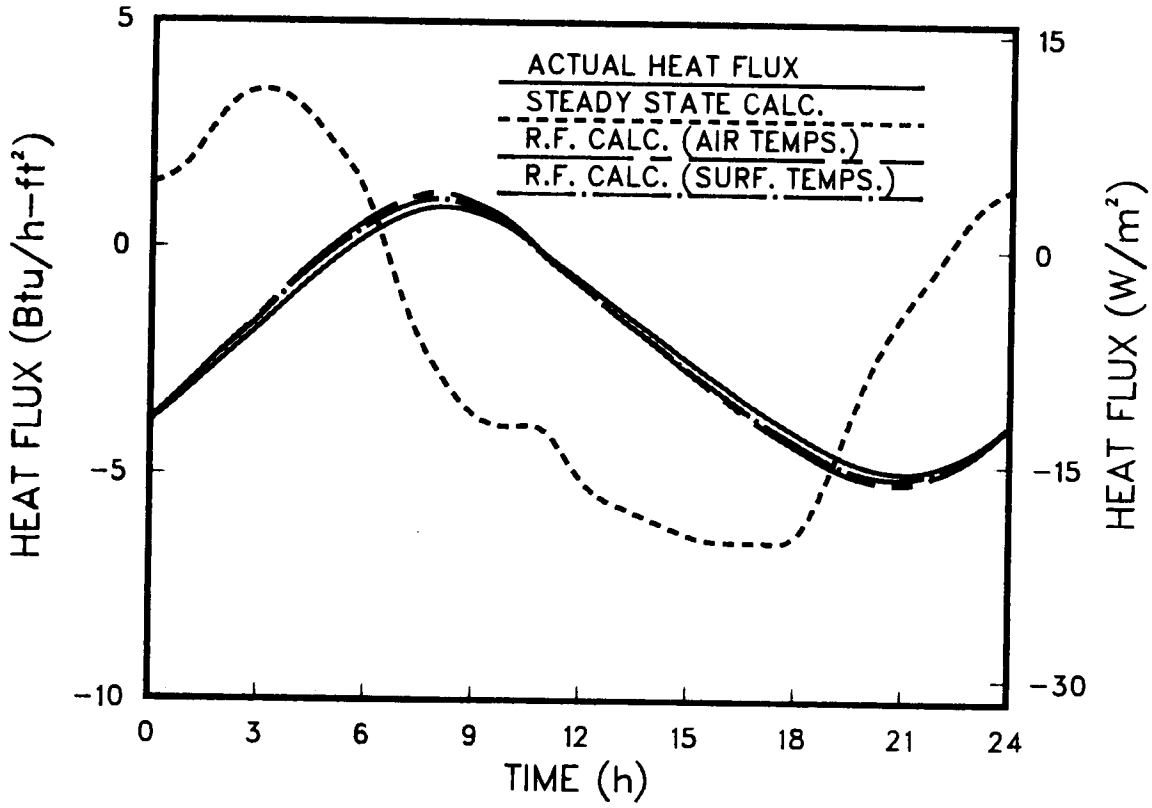

Fig. 13. Heat flux at inside surface of wall C3 - numerical experiment with an error in the inside surface temperature.

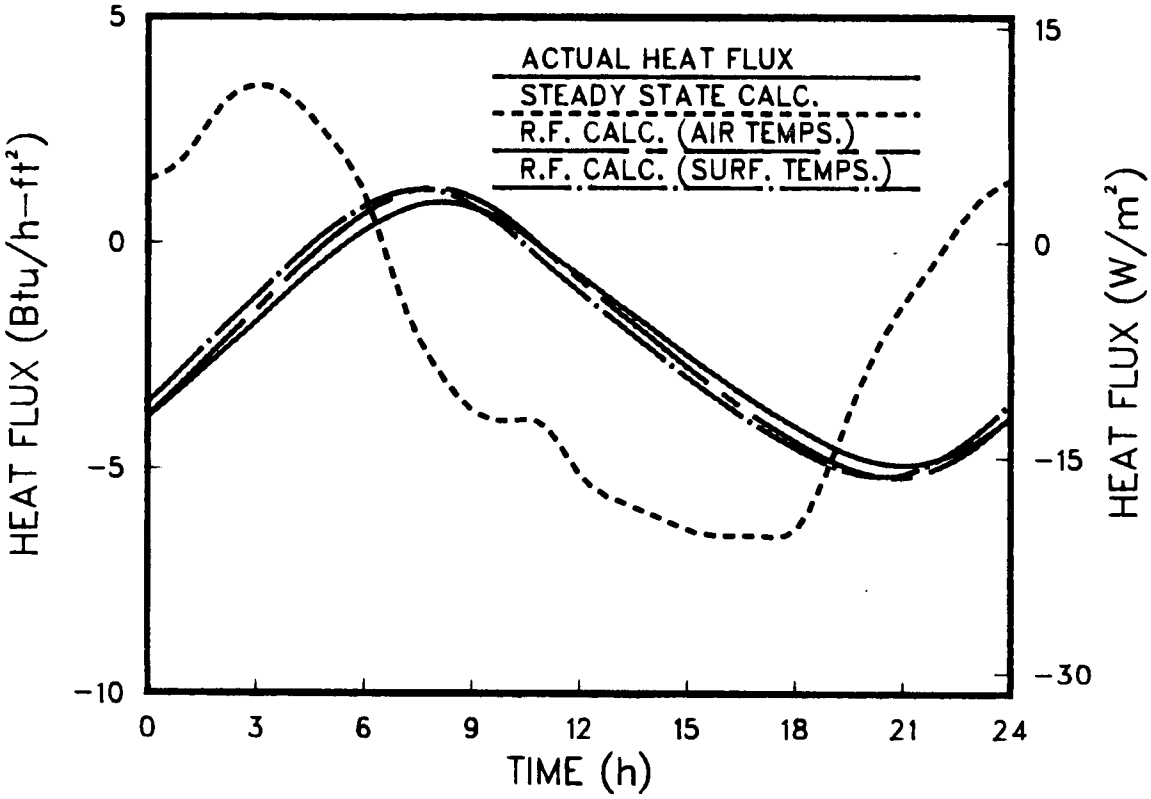

Fig. 14. Heat flux at inside surface of wall C3 - numerical experiment with an error in the outside surface temperature.

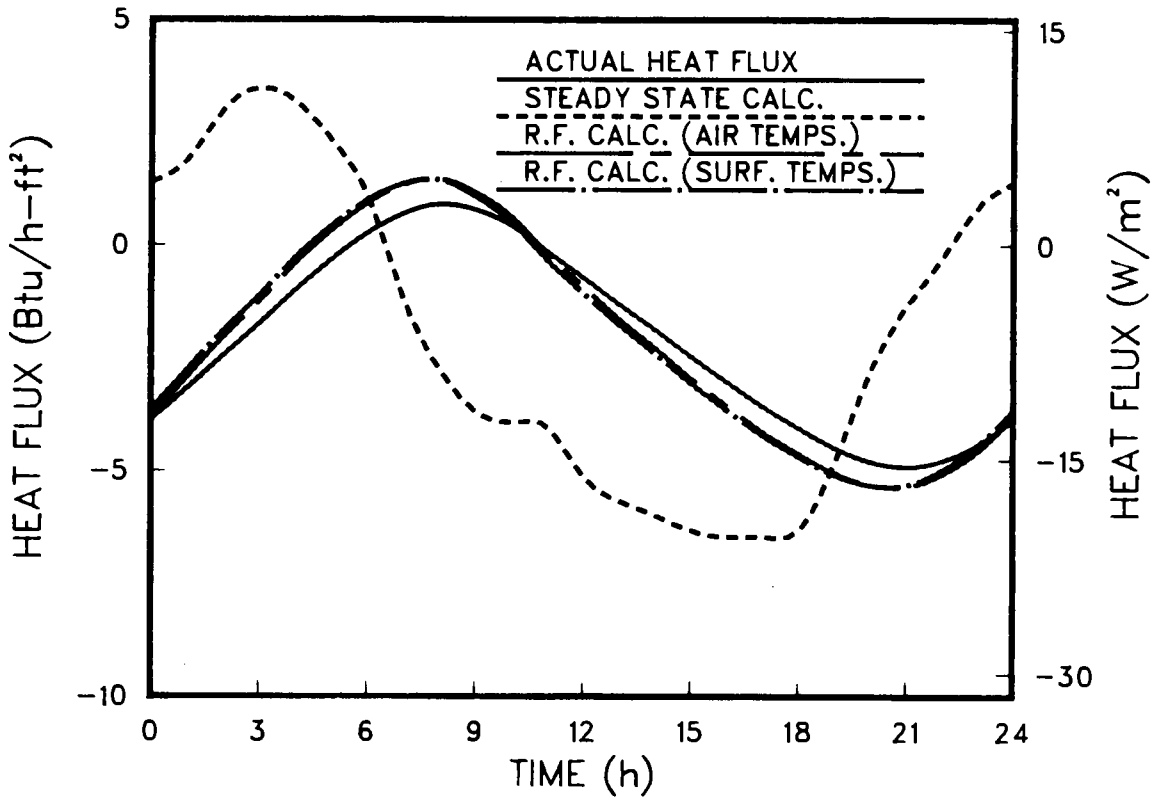

Fig. 15. Heat flux at inside surface of wall C3 - numerical experiment with errors in inside and outside surface temperature.

6. INFLUENCE OF WALL SURFACE TEMPERATURE ON FLOW PATTERNS

The velocity of the forced air flow across the faces of the wall is relatively low (approximately 1 ft/s). In the outdoor chamber the wall temperature is often 15°F above or below the air stream temperature during the cycle. This temperature difference can be even greater, depending on the particular temperature cycle being employed. In this range of temperature difference and with the low velocity forced air flow, natural convection can be of the same order of importance as forced convection in determining the surface heat transfer coefficient (or air film R value which is the reciprocal of the heat transfer coefficient). In the response factor calculations, the heat transfer coefficients are assumed to be constant. There will be an impact on the calculated results if they are actually a function of temperature.

To gain a better insight into the role that natural convection plays, a series of three calculations was performed using a finite difference computer program[8] to model the flow past the wall in the outdoor chamber. The flow in the channel adjacent to the test wall in the outdoor chamber enters at the bottom, makes a 90° turn aided by turning vanes, and flows in an upward direction past the test wall. The flow must then make another 90° turn to exit from the flow channel at the top. There is a wire grid in the flow stream to support the thermocouples measuring the air temperature. There are also thermocouple leads and heat flux transducer leads running across the face of the wall. All of these items have some influence on the flow in the channel. The flow is obviously quite complex, so no effort was made to model it exactly. The model was devised to maintain enough of the important characteristics of the actual flow so that the effect of the wall/air temperature difference on the actual flow could be inferred from the solution of a simpler case. The model is a two-dimensional slice through the channel. Any effects due to the sides of the hot box are not modeled. In the simplified model, the 90° turn at the channel entrance and the effect of any wires or other small features in the flow channel were not modeled. The 90° turn at the channel exit, as well as the dimensions of the channel, were maintained. The velocity profile imposed at the entrance was fully developed laminar flow. The peak velocity at the channel center was chosen so that the average velocity across the channel was 1 ft/s (0.3 m/s). Three cases differing only in the assumed wall surface temperature were run using this model. In all of the cases it was assumed that the wall was isothermal (i.e. there was no temperature variation vertically along the wall). The baffle dividing the flow channel from the rest of the outdoor chamber is also assumed to be isothermal. Its temperature is fixed at the same value as the entering air temperature.

Case 1 is a totally isothermal case which was run to serve as a base case for comparison. The entering air is at the same temperature as the wall. There is no heat transfer occurring in this case. Since the air will remain at the temperature at which it entered, there are no natural convection effects due to bouyancy. Cases 2 and 3 are identical to Case 1 except the wall temperatures are different than the inlet air temperature. Any differences between this Case 1 and either Case 2 or 3 are due solely to the wall temperature being different from the inlet air temperature. Figure 16 is a plot of streamlines for Case 1. The figure does not reflect the true aspect ratio of the channel because different scaling was used on the two axes. The vertical axis is the distance from the bottom of the hot box (Y) divided by the height of the hot box (H). The horizontal axis is the distance from the baffle (X) divided by the width of the channel (W). A streamline can be interpreted as being the path that the air follows as it flows through the channel. By plotting the path followed by the air entering the channel at several locations that are uniformly distributed across the channel entrance, an overall picture of the the flow within the channel can be established. Figure 17 shows the velocity profile in the channel at a height of 7.25 feet (2.2 m) from the entrance. This position is just below the channel outlet through the baffle defining the flow channel.

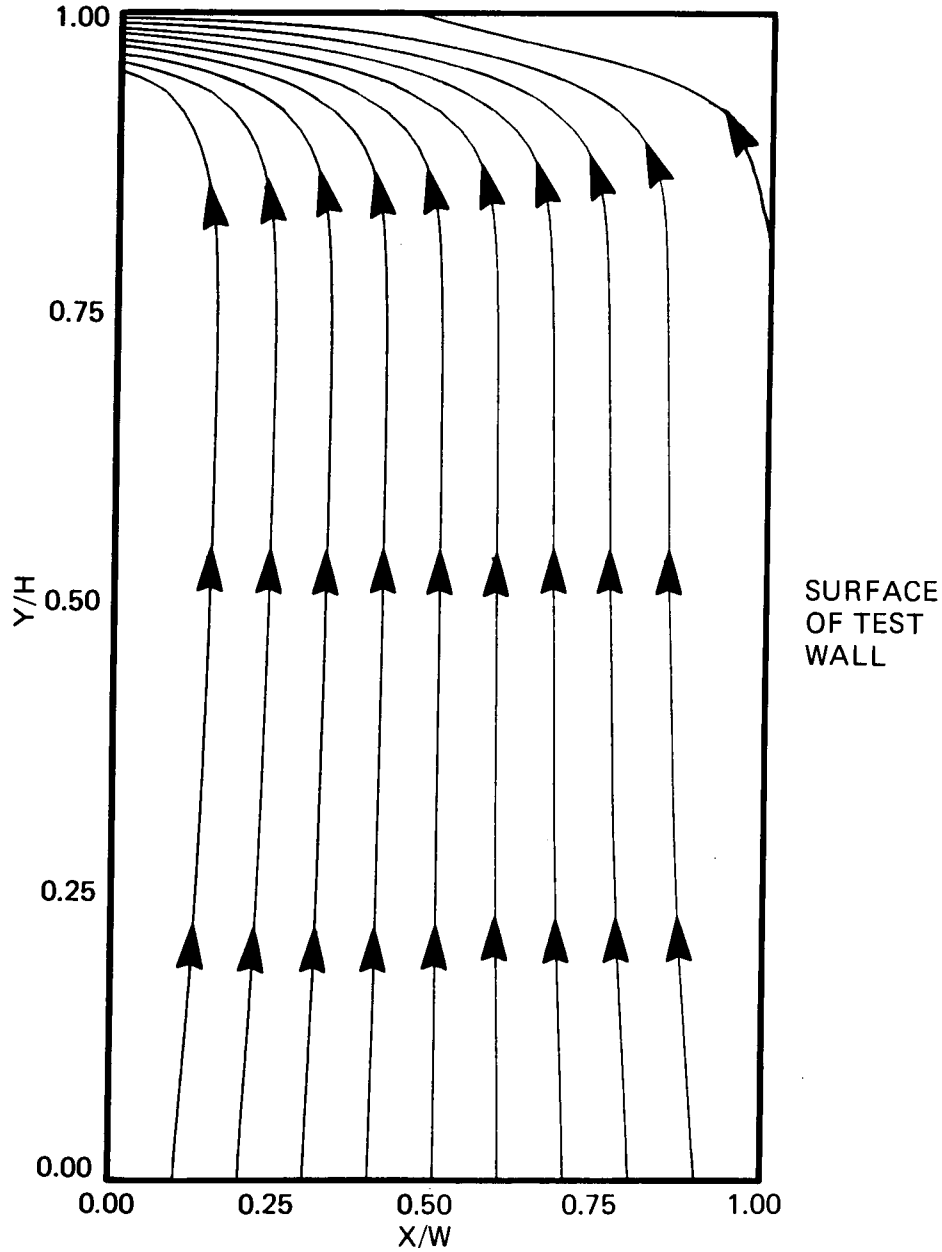

Fig. 16. Streamlines in outdoor flow channel - isothermal case.

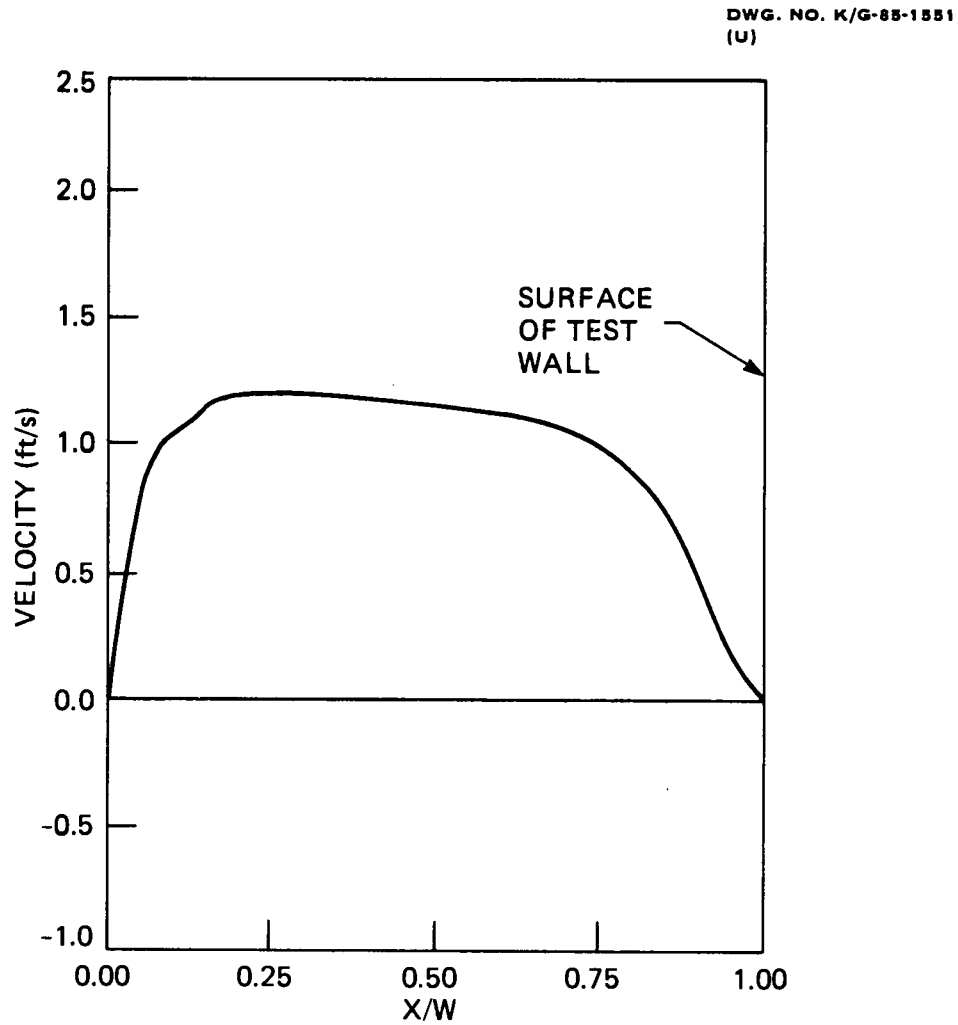

Fig. 17. Velocity profile in outdoor flow channel 7.25 feet from the entrance.

Case 2 is a hot wall case. It is identical to Case 1 except that the test wall surface temperature is now 10°F (5.6°C) above the inlet air temperature. Figure 18 presents the streamlines for this case. The overall flow pattern does not appear too dissimilar to that of Case 1. There is a slight, but clearly discernible, shift of the streamlines toward the wall in the upper portion of the channel. Figure 19 gives the velocity profile across the channel at a height of 7.25 feet (2.2 m) from the bottom. This profile is markedly different from that of Case 1. The warm wall has heated the fluid next to it, accelerating it due to bouyancy. Fluid has been drawn from the rest of the channel toward the wall as was observed in the plot of the streamlines. Figure 20 presents a plot of isotherms in the channel. There is a rather steep temperature gradient near the wall, but in most of the channel the temperature has not been influenced significantly by the wall.

Case 3 is a cold wall case in which the imposed wall temperature is 10°F (5.6°C) below the inlet air temperature. The streamlines for this case are presented in Fig. 21. The flow pattern is entirely different from that observed for either of the two previous cases. Even though the direction of the forced flow is upward, the actual flow over much of the test wall surface is downward for this case. The inlet streamlines move away from the wall as they go up the channel. A region exists near the wall in which the fluid recirculates and does not mix with the fluid flowing through the channel. Figure 22 is a plot of the velocity profile across the channel at a height of 7.25 feet (2.2 m) from the bottom. The negative (downward) velocity near the wall is quite pronounced. The magnitude of the maximum upward velocity is also significantly larger than in the previous cases since the effective channel width through which it flows has been reduced by the recirculation region. The isotherms for this case are given in Fig. 23. There are still steep temperature gradients near the test wall surface but the fluid temperatures well out into the channel have now been influenced by the wall.

One point is clearly made by the previous results: the test wall surface temperature can definitely impact the flow pattern in the channel adjacent to the test wall. Since the heat transfer coefficient is primarily determined by the velocity of the air flowing past the surface, it too is influenced by the surface temperature. What is not determined is how the heat transfer coefficient is affected or to what degree. In performing the response factor calculations from one air stream to the other, two values are needed to specify the boundary condition: the heat transfer coefficient and the air temperature. The air temperature that was used in the calculations was obtained from an average of the grid of thermocouples located 3 inches (7.6 cm) from the test wall in the flow channel. An examination of the isotherms of Figs. 20 and 23 suggests that this does not represent the fluid temperature that the wall is exposed too. This is particularly true of the case where the wall temperature is below the air temperature.

The effects discussed above may be less important in the actual hot box than is indicated by the calculations. Two elements of the hot box which were not included in the model, the 90° turn at the entrance and any features in the channel with small dimensions, will tend to induce turbulence and more thorough mixing of the fluid than the model indicates.

The hot box was not instrumented to study a phenomenon such as described here, so it is difficult to be definitive in establishing its significance or even its occurrence. The available data was nonetheless examined for any evidence that would either support or refute the possibility. As has already been mentioned, there are heat flux transducers mounted on the surfaces of the test wall. The values from these heat flux transducers were not used in the response factor calculations because they were considered less accurate than the energy balance on the indoor chamber. However, their behavior does probably reasonably reflect the relative change and time variation of the heat flux. The heat flux and temperature data for the outside surface of the normal weight concrete wall were examined for three dynamic tests. These tests were the NBS cycle, the NBS cycle plus 10°F, and the NBS cycle minus 10°F. A plot of surface heat flux versus temperature difference is presented in Fig. 24. The temperature difference is defined as the surface temperature

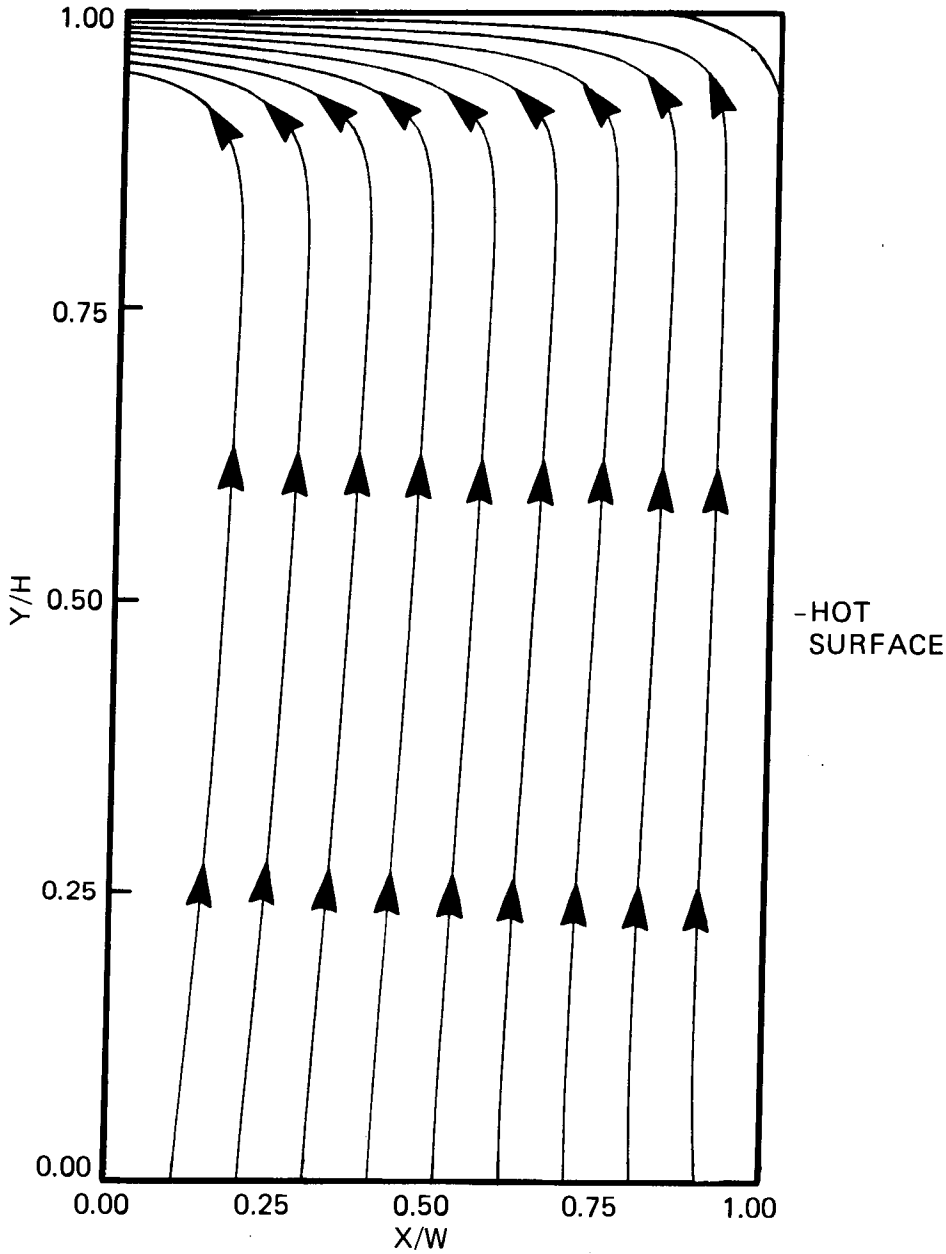

Fig. 18. Streamlines in outdoor flow channel - hot wall case.

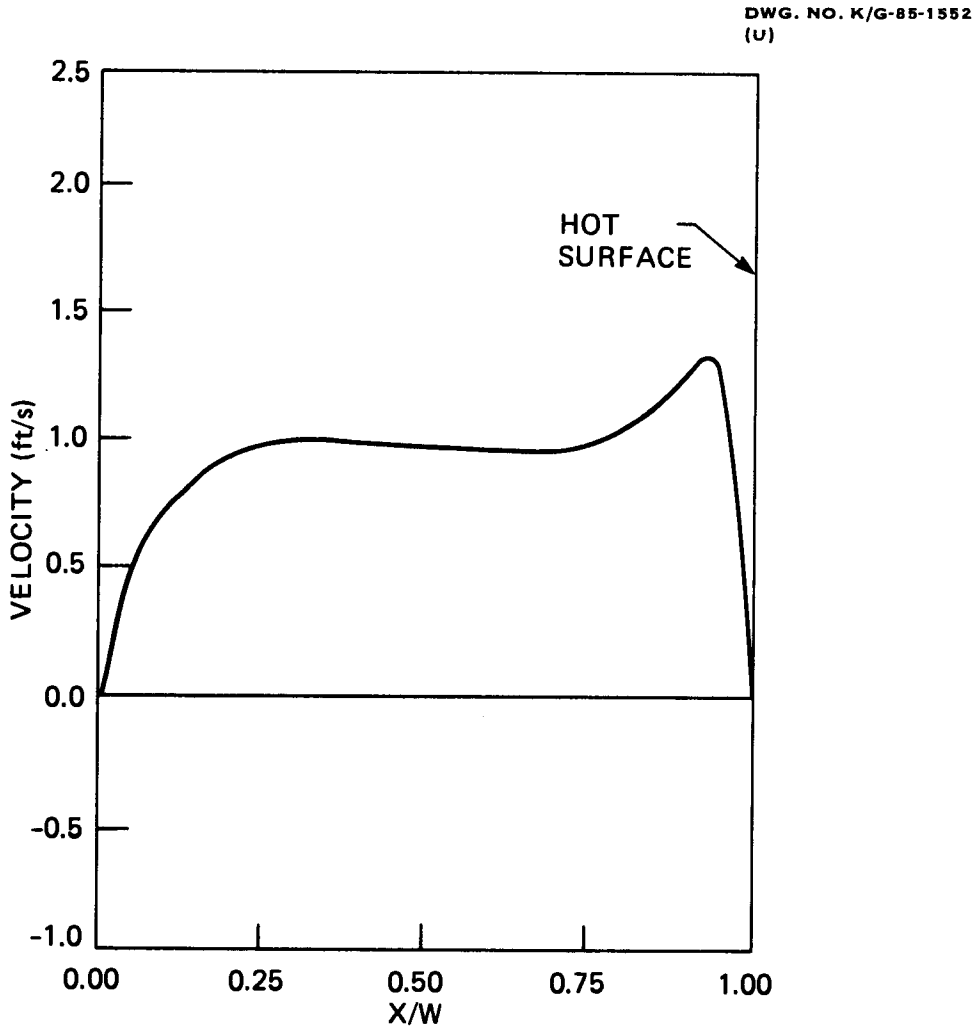

Fig. 19. Velocity Profile in outdoor flow channel 7.25 feet from the entrance - hot wall case.

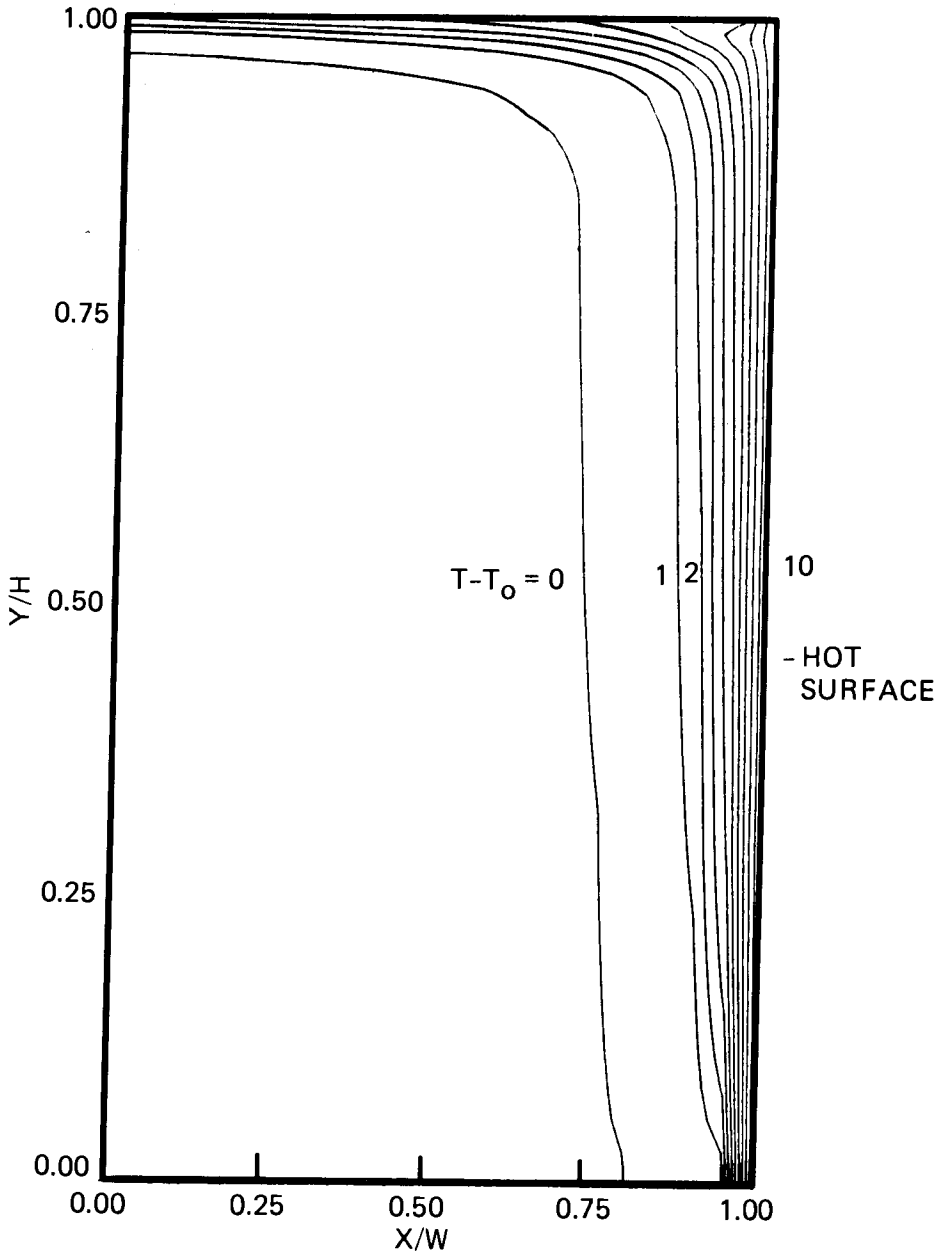

Fig. 20. Isotherms in outdoor flow channel - hot wall case.

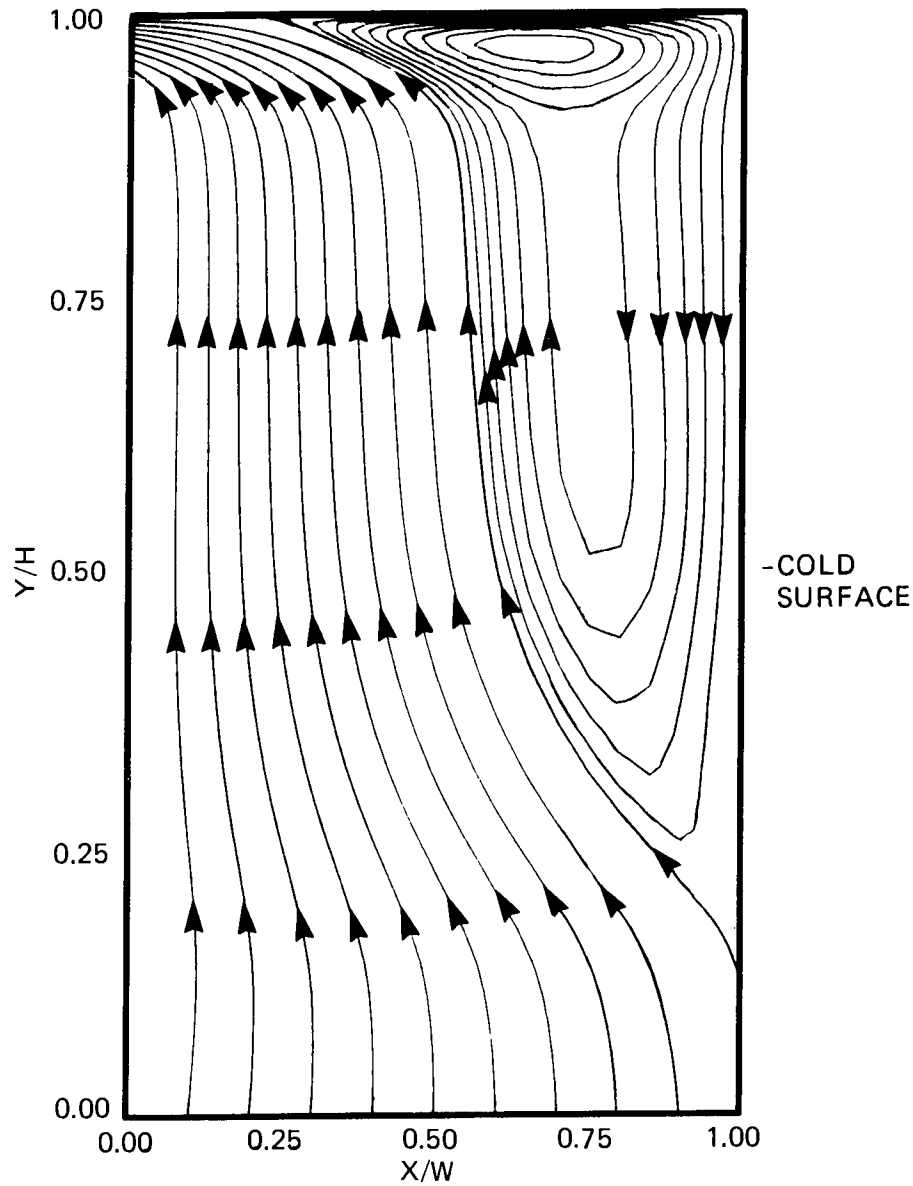

Fig. 21. Streamlines in outdoor flow channel - cold wall case.

DWG. NO. K/G-85-1553
(U)

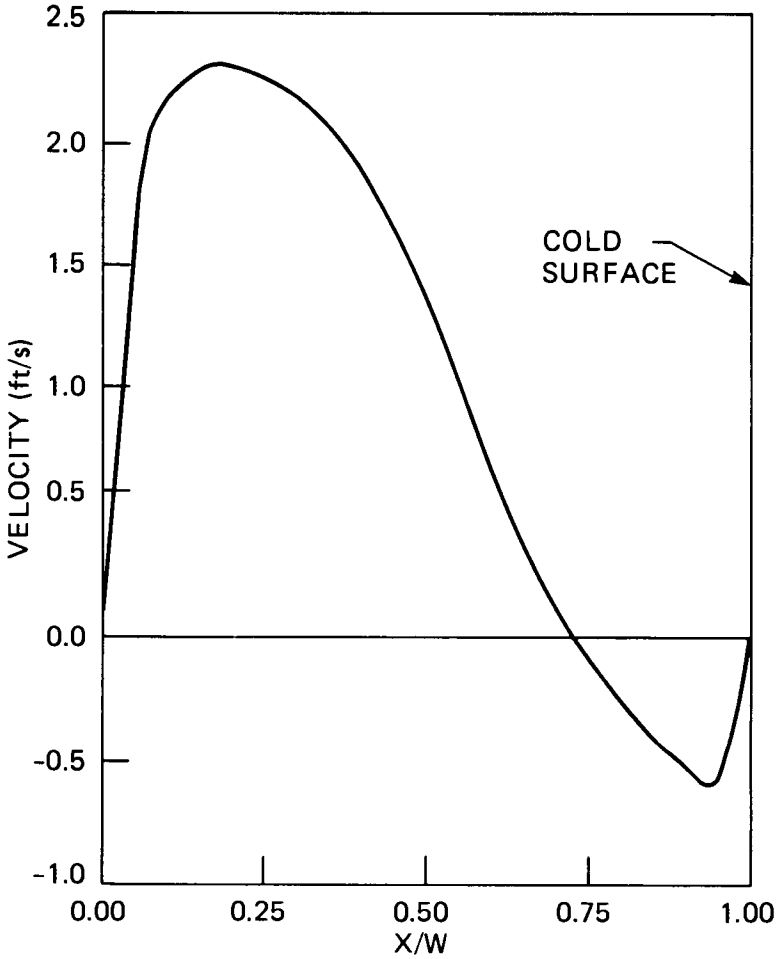

Fig. 22. Velocity profile in outdoor flow channel 7.25 feet from the entrance - cold wall case.

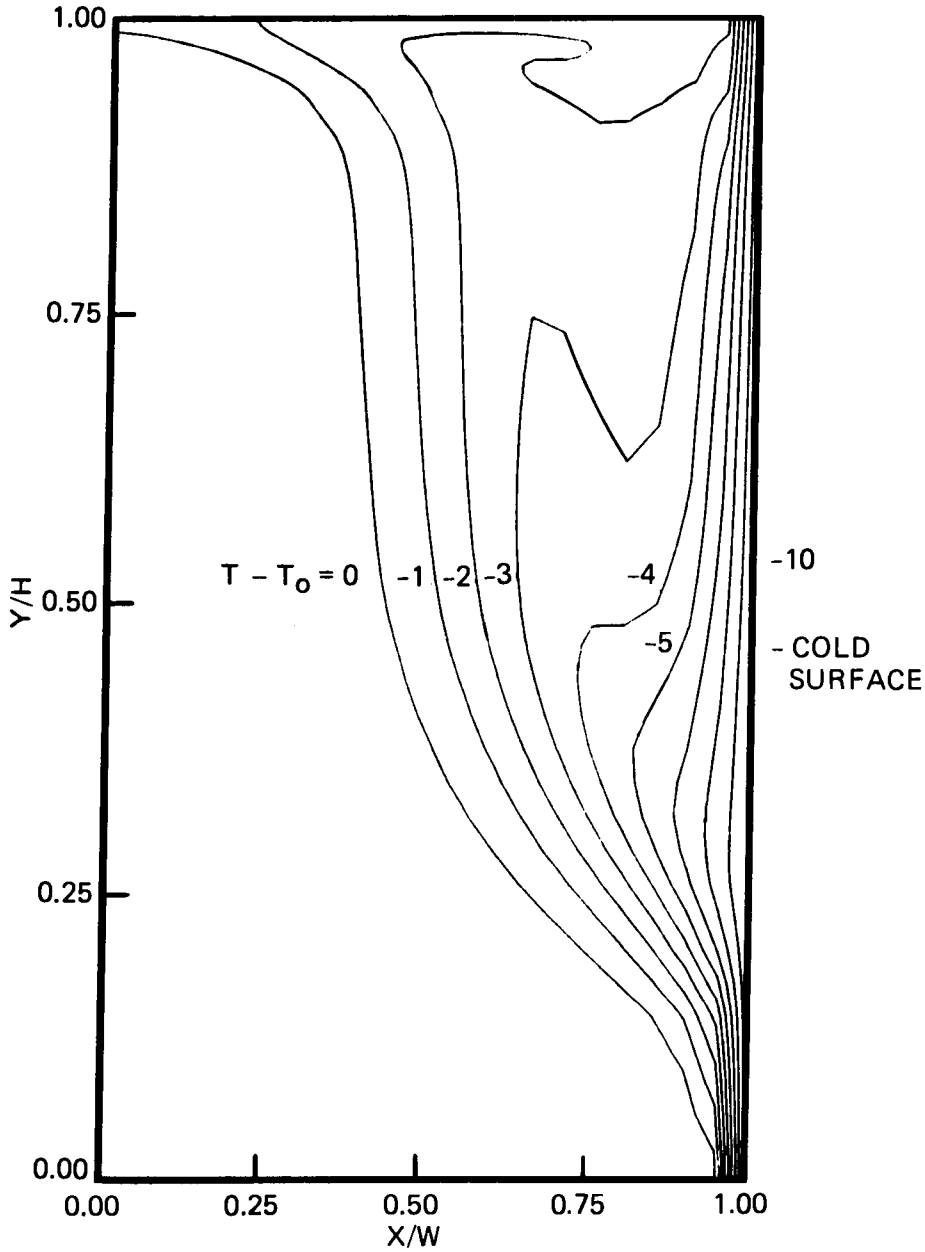

Fig. 23. Isotherms in outdoor flow channel - cold wall case.

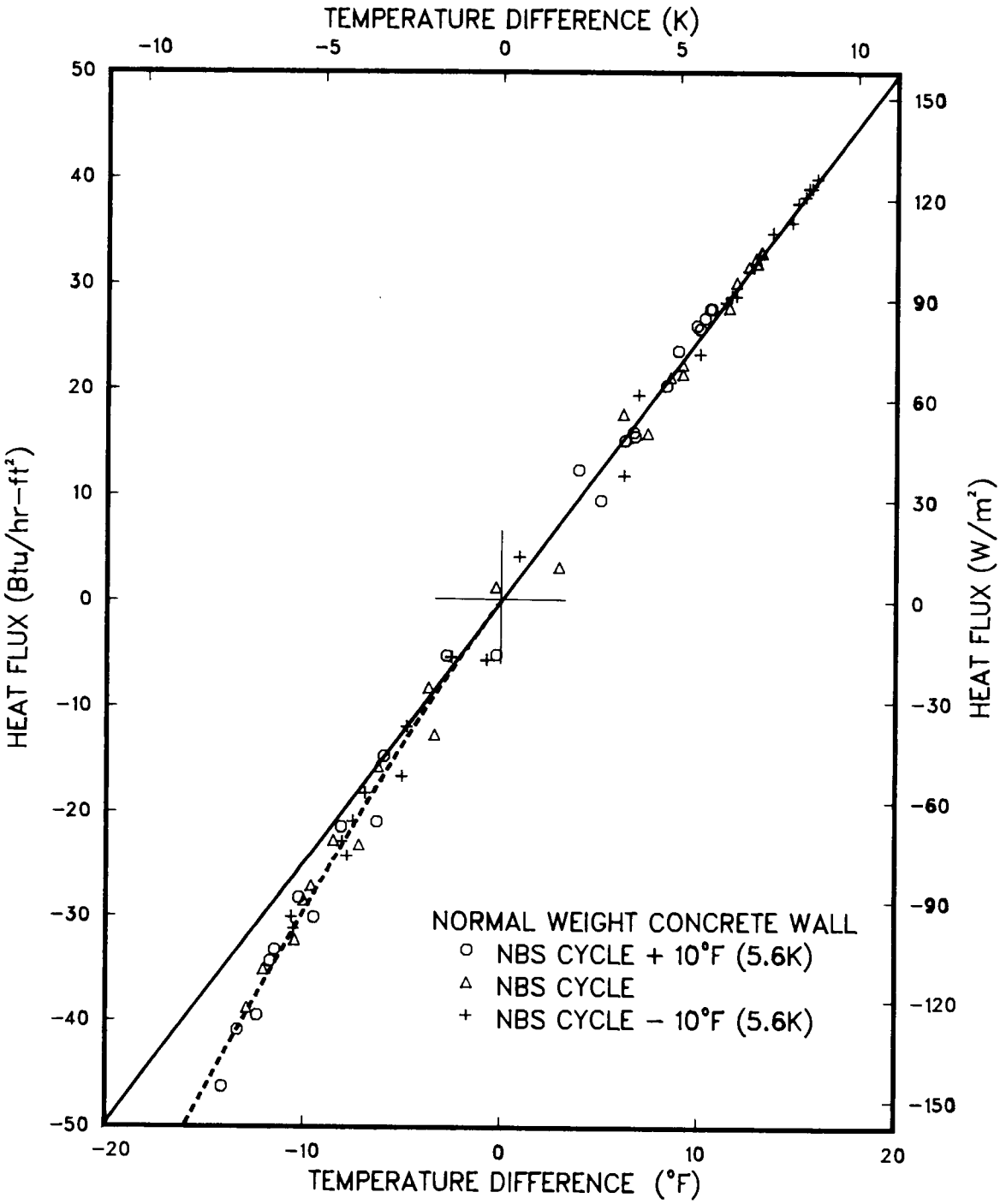

Fig. 24. Heat Flux at outside surface of wall C1 versus surface/air temperature difference.

minus the air temperature. A positive temperature difference indicates the wall surface is warmer than the air, and a negative temperature difference indicates it is cooler than the air. If the heat transfer coefficient is a constant, all of the data should fall reasonably close to a straight line passing through the origin (0,0). The solid line in the figure is a straight line passing through the origin that has been fit by applying the least squares method to all of the data for which the temperature difference is positive. The slope of this line is by definition the heat transfer coefficient. For the data with a positive temperature difference, this line is a reasonable fit of the data. At small values of temperature difference, there is some scatter observed, but as the temperature difference increases there is very little scatter in the data. However, the data points for negative temperature differences do not fall on this line. In fact the greater the magnitude of the negative temperature difference the greater the deviation from the straight line. The best fit of the data with negative temperature differences was not obtained with a straight line but with a curved line. This fit is shown as the dashed line in Fig. 24. This is strong evidence that the heat transfer coefficient is not a constant. The influence of the surface/air temperature difference is the probable cause of this deviation from a straight line.

An interesting aspect of the data presented in Fig. 24 is the fact that the greatest scatter occurs at small temperature differences. Based on data points for which the temperature difference is very near zero, a temperature difference of zero does not result in a zero heat flux. Physically this cannot be the case so there must be an explanation for this behavior. To better understand what was occurring, the data for each of the three different cycles were plotted separately in Figs. 25, 26, and 27. Arrows are included on these plots connecting data points to indicate the time sequence in which they occurred. By plotting the data in this way, it becomes evident that there is a hysteresis effect possibly due to a lag in the response of the heat flux transducer. When the temperature difference approaches zero from above the heat flux at zero temperature difference is positive; when approached from below it is negative. However, the hysteresis is not the same when approached from above as it is when approached from below, as would be expected if it was due solely to a lag in the response of the transducer. There is a larger discrepancy when approached from below. The flow pattern goes through transitions in which a recirculation region is established and later dissipates during each repetition of the cycle. If there is indeed a recirculation region in the flow field when the temperature difference is negative, then what is being observed may be due to a mass of air being trapped near the wall. The wall is responding to the temperature of the trapped air rather than to the temperature of the air entering the channel. At the present time this is simply speculation since there is no clear evidence that it is in fact true.

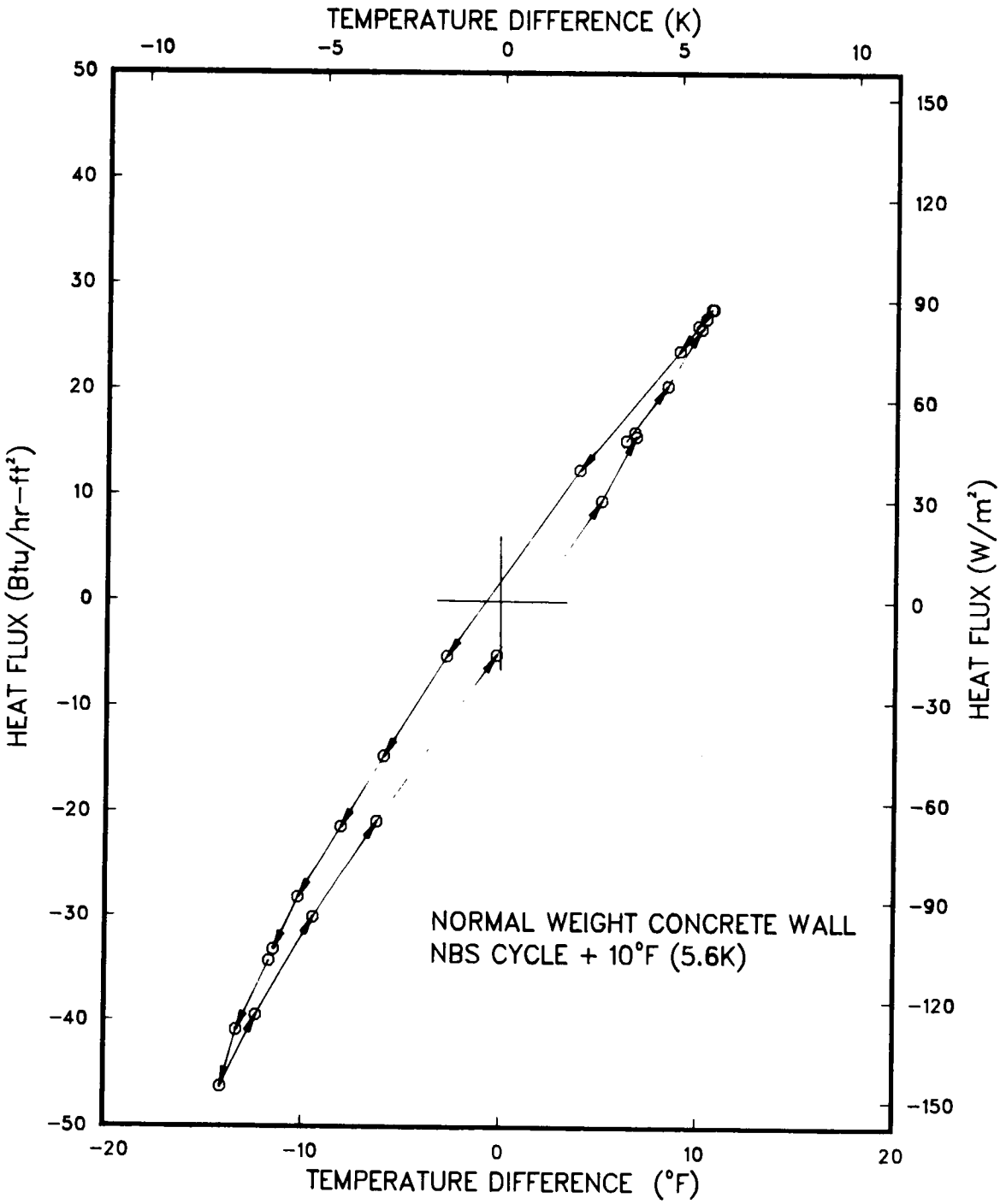

Fig. 25. Heat flux at outside surface of wall C1 versus surface/air temperature difference - NBS cycle + 10°F.

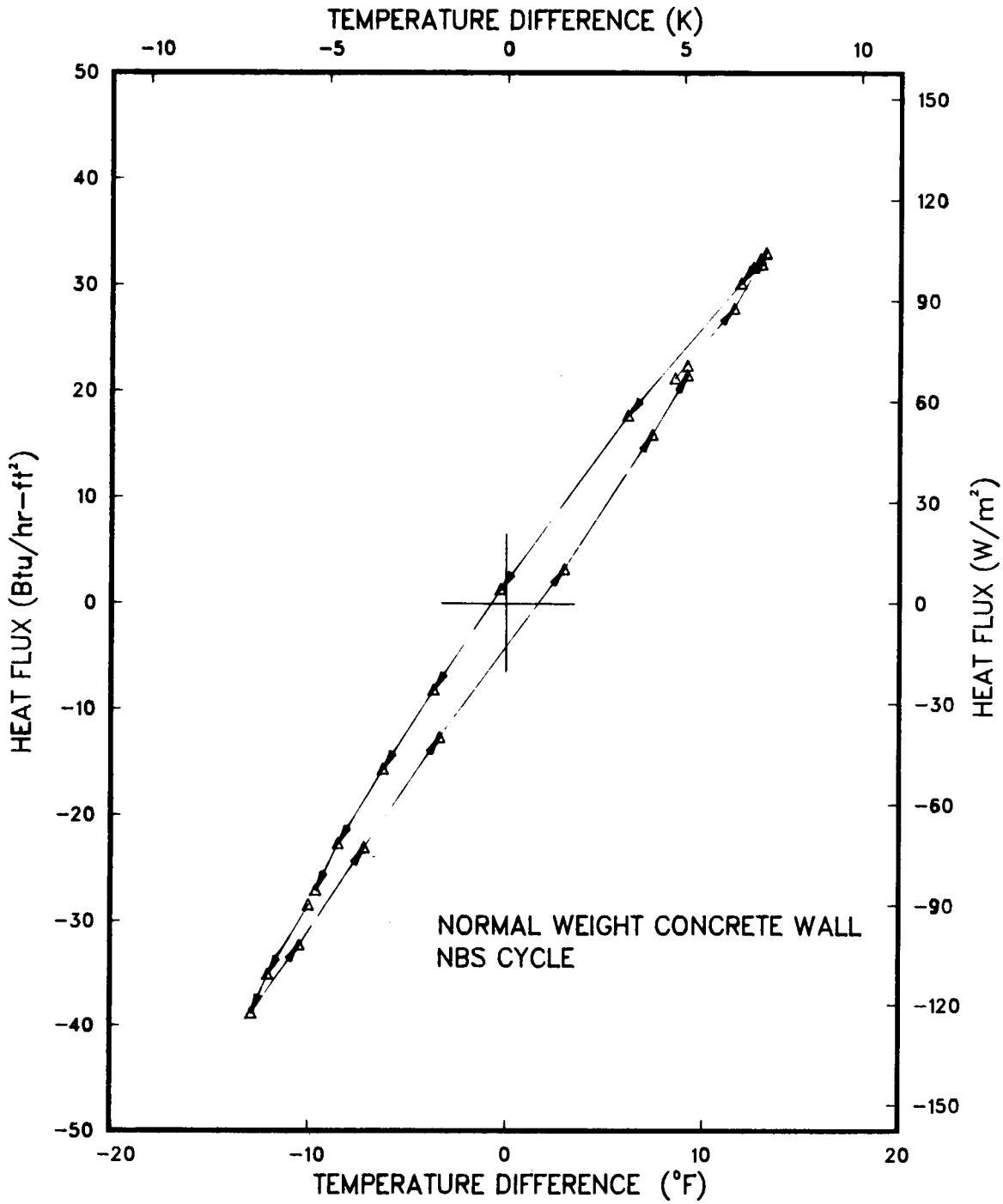

Fig. 26. Heat flux at outside surface of wall C1 versus surface/air temperature difference - NBS cycle.

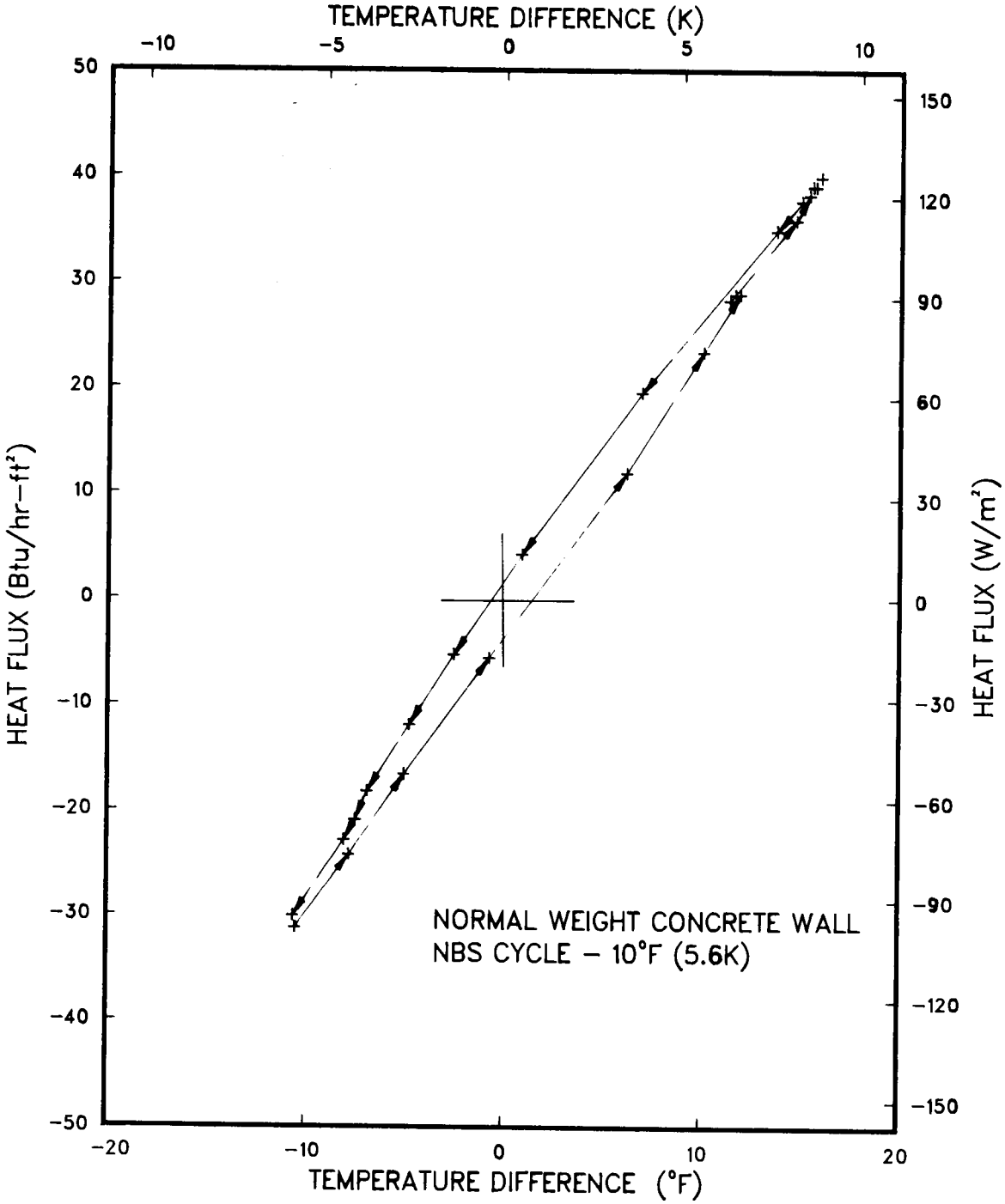

Fig. 27. Heat flux at outside surface of wall C1 versus surface/air temperature difference - NBS cycle - 10°F.

7. INFLUENCE OF THE MASS OF THE CALIBRATED HOT BOX

Thus far in the investigation of the calibrated hot box data there has not been an argument presented that can explain why the time lag observed in the experiments is so much greater than the lag predicted analytically. One possible explanation is that the hot box itself is introducing a lag in addition to that produced by the test wall. In the indoor chamber, the conditioned air enters the flow channel adjacent to the test wall at the top and flows downward. As it flows past the wall, it picks up heat from, or loses heat to, the test wall. The flow then exits from the bottom of the channel into the indoor environmental chamber. At this point a detailed energy balance on the air entering and leaving the flow channel should theoretically give an accurate indication of the heat flow at the inside surface of the test wall. In the indoor environmental chamber the air comes in contact with and exchanges heat with all chamber surfaces, the conditioning equipment, the instrumentation, and any other mass present. The air is then drawn into a conditioning plenum where heat is added or removed in order to return the air to the setpoint temperature. This energy added or removed at the conditioning plenum is interpreted as being the energy that has been transfered from the wall to the air; however, it is actually the net energy change resulting from heat transfer between the test wall, the air, and other mass in the indoor chamber of the hot box.

The phenomenon just described can produce an additional lag in the observed heat flow at the inside surface of the test wall. Consider, for example, a situation in which the outdoor chamber air temperature undergoes a step increase to a value above the fixed indoor temperature. When the effects of this first reach the inside surface of the test wall, the air flowing down the channel adjacent to the wall will increase in temperature to a value above the indoor setpoint. The air exiting the flow channel is warmer than the surfaces of the indoor environmental chamber and will lose heat to them. Thus, the air entering the conditioning plenum is not at the same temperature as it was when it left the flow channel adjacent to the test wall. The heat that has to be removed from the air in the conditioning plenum is not equal to that coming through the test wall at that particular time. The mass of the indoor chamber and its contents has introduced a delay in the time that a change in the heat flow through the wall will be detected at the conditioning plenum. The same type of delay that occurs in the step transient will also occur in the steady periodic dynamic tests .

A simple analytical model was devised to obtain an estimate of the order of magnitude of any delay produced by the hot box itself. The heat flux at the inside surface of the test wall was assumed to be a steady periodic sine wave, thus eliminating the test wall from the simple model. The temperature of the air exiting the flow channel and entering the indoor environmental chamber is also sinusoidal and in phase with the heat flux at the test wall. Since the lining on the interior of the indoor chamber is thin and has a large surface area, a lumped capacitance model of the indoor chamber seems appropriate. It should be recognized that the lumped capacitance analysis will overestimate the effect of the mass of the hot box, and will thus give an upper bound on the additional lag rather than a best estimate of it. This simple model has an exact analytical solution for the temperature of the air exiting the indoor chamber and entering the conditioning plenum. By comparing the phase angle of the air temperature exiting the flow channel to that of the air entering the conditioning plenum, the lag produced by the chamber itself can be determined.

Results from the exact analytical solution are presented in Fig. 28 for a cycle of twenty-four hours. The lag produced by the mass of the hot box is characterized by two non-dimensional quantities. One of these is the ratio of the product of the mass flow rate ($\dot{m}$) and specific heat (c_p) of the air to the product of the convective heat transfer coefficient (h) and the total surface area (A) in the indoor chamber. The second quantity is the ratio of the sum of the products of density (ρ), specific heat (c_p), and volume (V) for all the masses in the indoor chamber to the product of the heat transfer coefficient and the surface area. To obtain an estimate of the lag that is present in the actual hot box the following assumptions were made: (1) the only mass in the interior chamber affecting the lag is the liner of the box which has an area of 174.25 ft^2 (16.2m^2) and a

DWG. NO. K/G-85-3817
(U)

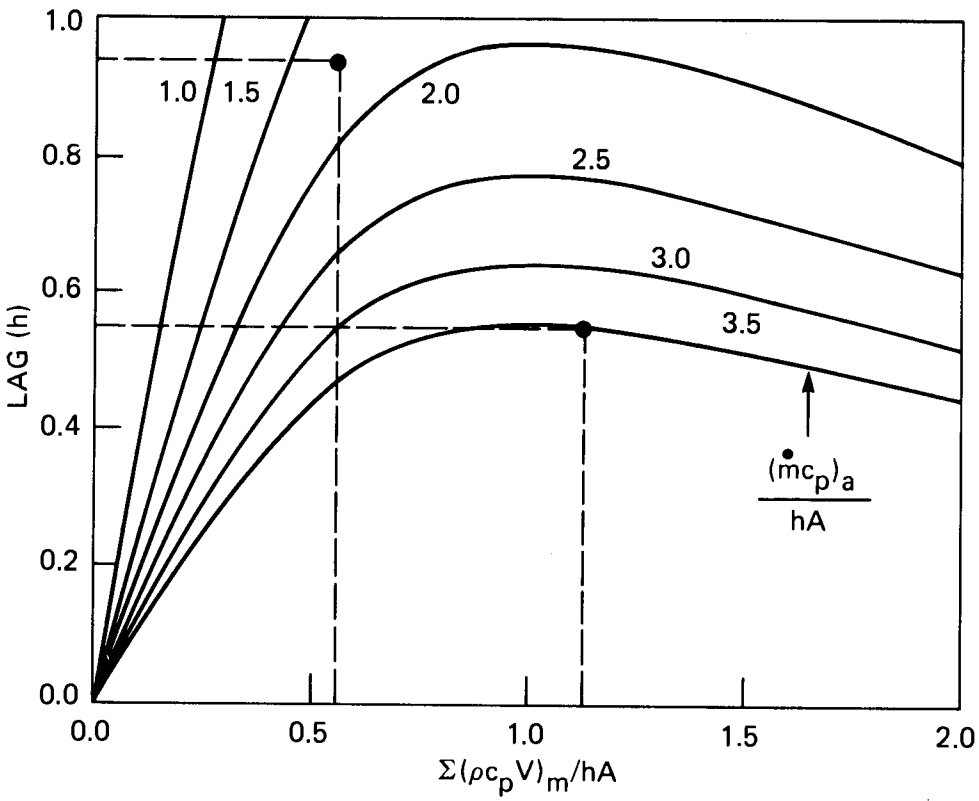

Fig. 28. Influence of hot box mass on observed lag in heat flux at inside surface of test wall.

volume of 5.45 ft^3 ($0.154m^3$), (2) the density and specific heat of the liner are 30 lb/ft^3 (480 kg/m^3) and 0.6 Btu/lb-°F (2500 J/kg-K), respectively, (3) the heat transfer coefficient is 1 Btu/h-ft-°F ($5.7W/m^2$-K), and (4) the volumetric flow rate of air is 280 ft^3/min ($0.13m^3/s$) at an average temperature of 70°F (21°C) resulting in a mass flow rate of 1254 lb/h (0.158 kg/s). With these assumptions the analytical model gives a value of the lag produced by the hot box as 0.94 hours. If the heat transfer coefficient is assumed to be 0.5 Btu/h-ft^2-°F (2.8 W/m^2-K) the lag is 0.55 hours.

There is additional mass in the interior chamber other than the liner. If this were included in the calculation a larger lag would be predicted. Also any radiative heat transfer from the test wall directly to the baffle defining the flow channel does not show up immediately as an increase in the air temperature. However, it needs to be recognized that the most one can hope to glean from this calculation is an indication whether or not there is a lag produced by the hot box itself, not an accurate prediction of the lag. It does appear feasible that the hot box may produce a lag on the order of a fraction of an hour. A comparison of the heat flux measured by the heat flux transducers on the inside surface of the test wall to that determined from an energy balance on the indoor chamber does not reveal a phase difference. However, since the heat flux data are available only at hourly intervals, lags produced by the hot box of much less than an hour may not be discerned. Whether or not the hot box actually does produce a lag cannot be satisfactorily determined with the current data.

One thing that can be concluded is that any lag produced by the hot box is not strongly dependent on the wall being tested. The hot box cannot be responsible for the difference between observed and calculated lags for all three of the test walls since this difference varies from wall to wall and is much greater than one hour for two of the walls.

8. INFLUENCE OF UNCERTAINTY IN WALL PROPERTIES

The most likely source for the difference between measured and calculated lag now seems to be in either one of two areas. First, the thermal properties of the wall being used in the calculations are in error; or, second, there is some heat transfer phenomenon other than conduction taking place in the test walls. The wall properties of interest are the conductivity, density, and specific heat. An error in the conductivity has already been explored to some degree in the section "Effect of Errors in Surface Temperature Measurements." In any event, an error in the conductivity cannot produce the observed difference in lag.

In the calculations, the density and specific heat never occur independently of each other. The quantity that appears is the product of the density and specific heat. An error in this product can produce the observed behavior. The measurement of the density of the wall is very straight forward, and it seems unlikely that a significant error could have been made in determining this quantity. The determination of the specific heat of a concrete sample is more involved, and an error in its determination seems more likely. The specific heat is determined by a technique similar to the Army Corp of Engineers Specification CRD-C124-73, Method of Test for Specific Heat of Aggregates, Concrete, and Other Materials (Method of Mixtures)[9,10]. In this method the concrete is ground up and tested in a saturated state. The resulting specific heat is then corrected for moisture content.

To determine if an error in specific heat can explain the observed behavior, a series of computer runs was performed in which the specific heat was varied. These showed that lags and amplitude reductions similar to those observed experimentally can be produced by the response factor calculations if the specific heat is increased to an appropriate value. To ascertain if a single value of specific heat for each wall can reproduce the measured heat fluxes for all of the cycles, a computer program was written to determine the value of the specific heat that gives the best fit (in a least squares sense) between the measured and calculated heat fluxes. A specific heat was determined from the data for each of experimental tests with this computer program. In all cases the specific heat determined from the fit produced a good match between calculated and measured

heat fluxes. Also in all cases the calculated specific heat was larger than the experimentally determined value. However, this process did not produce a single value of specific heat for each wall. The calculated values of specific heat were different for different test cycles, and were also different for the same test cycle depending on whether the calculations were done using air temperatures or surface temperatures. One possible explanation of this difference is the presence of more water in the concrete than was accounted for in making the moisture content correction to the specific heat, but it seems unlikely that an error large enough to cause the observed discrepancy could occur.

An error in the measured value of the specific heat seems a likely cause of the observed discrepancy between the calculated and measured heat fluxes, but it is not possible to make a conclusive statement that this is the actual cause based on the available data.

Another explanation for the observed discrepancy may be that there is another phenomenon besides conductive heat transfer occurring in the wall that manifests itself in a manner similar to that of a higher specific heat. A phase change occurring in the wall would produce just this effect. An obvious phase change that does occur in the wall is the transition of water between the liquid and vapor phases; but the amount of water that can change phase does not represent sufficient energy storage to account for the effect. Another phase change that may occur in these walls is the transition between water bound as a hydrate and free water. It has been suggested that the energy associated with this transition is much greater than that associated with the transition between the liquid and vapor phases. This is only offered as a hypothesis for consideration and is beyond the scope of this report. It was not pursued further at this time, though it might prove an interesting line of investigation for the future.

The fact that the walls are not truly homogeneous (they contain a layer of steel reinforcement near their midplane) was ruled out as contributing to the observed differences. Results from the response factor program in which a continuous layer of steel was included at the midplane of the wall did not differ significantly from the results for the homogeneous wall. Since the actual steel reinforcing is not a continuous layer, it would have even less impact.

9. CONCLUSIONS AND RECOMMENDATIONS

The heat flux at the inside surface of a test wall that was calculated using a response factor technique does not show good agreement with the experimental values obtained from hot box tests. Based on the results of this study, it was not possible to conclusively identify the source of the disagreement. However, the analysis did suggest several possible sources of error. One of these is an error in measuring the surface temperature of the test wall. Discrepancies resulting from such an error would not be too significant in cases where the resistances due to the air films are small compared to the test wall R value. A vast majority of the walls that will be tested in a calibrated hot box will have a much larger R value than the concrete walls in this study. In general, this may not be an area of concern, but for the testing of low R value walls it does need to be considered. There are techniques available that will reduce this type of error. These include the use of smaller gauge wire for the thermocouples and embedding the thermocouple junction and its leads into the surface of the wall. It is probably worthwhile to take these precautions when testing low R value walls.

Another potential source of error that was identified is the influence of the test wall temperature on the flow pattern, and consequentially the surface heat transfer coefficient. Once again if the resistance due to the surface air films is small in comparison to the test wall R value, this may not be of much consequence. However, for low R value wall tests this may introduce enough uncertainty in the results to make them difficult to interpret. A greater mass flow rate may be necessary. This is an area which should be investigated further.

The mass in the indoor chamber of the hot box may introduce a slight lag in the observed heat flux. While this does not appear to be very significant, it is another source of uncertainty when one attempts to interpret the results. It would be beneficial to collect data on a more frequent schedule than hourly in order to definitely resolve the issue. If the mass of the hot box does turn out to introduce a lag, an appropriate correction could be applied to the results or measures could be taken to minimize the effect.

The most likely cause of the observed discrepancy between the measured and calculated heat flux is the value used for the specific heat of the concrete. It seems likely that either the measured value of specific heat is not correct or there is a phase change process occurring in the wall. If there is a phase change occurring, it could be handled by using an effective specific heat rather than the actual value in the calculations. The value of specific heat that was used in this study for the normal weight concrete wall is not unlike the values normally used in most analyses of building energy use. Therefore, this issue has implications ranging far beyond the analysis of the data for the current study. This is an area that definitely needs further investigation.

ACKNOWLEDGMENTS

The work presented in this report was done as part of the National Program for Building Thermal Envelope Systems and Materials. The research was sponsored by the Office of Buildings and Community Systems, Building Division, U. S. Department of Energy. The data used in the analyses came from the calibrated hot box at the Construction Technology Laboratories of Skokie, Illinois. Dr. Anthony E. Fiorato and Martha G. VanGeem of the Construction Technology Laboratories were helpful in providing and interpreting the hot box data. The fluid calculations presented in this report were performed by J. N. Tunstall of the Computing and Telecommunications Division, Martin Marietta Energy Systems. Special appreciation is extended to L. W. Winborn who prepared this report for publication.

REFERENCES

1. Fiorato, A. E., "Laboratory Tests of Thermal Performance of Exterior Walls," Proceedings of the ASHRAE/DOE-ORNL Conference on Thermal Performance of the Exterior Envelopes of Buildings, Orlando, Florida, Dec. 1979, ASHRAE SP28, New York, 1981, pages 221-236.

2. Van Geem, M. G., et. al., "Heat Transfer Characteristics of a Normal-Weight Concrete Wall," Construction Technology Laboratories, Portland Cement Association, Skokie, Illinois, Feb. 1983.

3. Van Geem, M. G., Fiorato, A. E., "Heat Transfer Characteristics of a Structural Lightweight Concrete Wall," Construction Technology Laboratories, Portland Cement Association, Skokie, Illinois, June 1983.

4. Van Geem, M. G., Fiorato, A. E., "Heat Transfer Characteristics of a Low Density Concrete Wall," Construction Technology Laboratories, Portland Cement Association, Skokie, Illinois, Aug. 1983.

5. Peavy, B. A., Powell, F. J., and Burch, D. M., "Dynamic Thermal Performance of an Experimental Masonry Building," Building Science Series 45, U. S. Department of Commerce, National Bureau of Standards, Washington D. C., July 1973.

6. Peavy, B. A., "Determination and Verification of Thermal Response Factors for Thermal Conduction Applications," NBSIR 77-1405, U. S. Department of Commerce, National Bureau of Standards, Washington D. C., April 1978.

7. Elrod, D. C., Giles, G. E., and Turner, W. D., "HEATING6: A Multidimensional Heat Conduction Analysis with the Finite-Difference Formulation," ORNL/NUREG/CSD-2/V2, Oak Ridge National Laboratory, October 1981.

8. Tunstall, J. N., Park. J. E., "Two-Dimensional Modeling for Compressible, Slightly Three-Dimensional Flows," report in preparation.

9. Whiting, D., Litvin, A., and Goodwin, S. E., "Specific Heat of Selected Concretes," Journal of the American Concrete Institute, July 1978, pages 299-305.

10. "Method of Test for Specific Heat of Aggregates, Concrete, and Other Materials (Method of Mixtures)," Handbook for Concrete and Cement, U. S. Army Waterways Experiment Station, Vicksburg, Mississippi, CRD-C124-73.

INTERNAL DISTRIBUTION

1. R. S. Carlsmith
2-5. K. W. Childs
6. J. E. Christian
7. G. E. Courville
8. F. A. Creswick
9. J. S. Crowell
10. W. Fulkerson
11. G. E. Giles
12. T. S. Lundy
13-22. M. C. Matthews
23. D. L. McElroy
24. H. McLain
25. J. W. Michel
26. W. R. Mixon
27-29. D. S. Napolitan
30. J. P. Sanders
31. A. C. Schaffhauser
32. J. N. Tunstall
33. G. E. Whitesides/R. P. Leinius
34. L. W. Winborn
35. A. J. Witten
36. Central Research Library
37. Document Reference Center
38-40. Laboratory Records
41. Laboratory Records (RC)
42. ORNL Patent Office

EXTERNAL DISTRIBUTION

43. C. D. Auburg, DOE, Bonneville Power Admin., Portland, OR
44. C. G. Bankvall, Swedish National Testing Institute, Boras, SWEDEN
45. J. J. Boulin, DOE/CE, Washington, DC
46. W. C. Brown, National Research Council of Canada, Ottawa, Ontario, CANADA
47. H. W. Busching, Clemson University, Clemson, SC
48. J. H. Cable, John Cable Associates, Inc., Alexandria, VA
49. T. J. Cardenas, Steven Winter Associates, New York, NY
50. W. Carroll, Lawrence Berkeley Laboratory, Berkeley, CA
51. R. S. Dougall, University of Pittsburgh, Pittsburgh, PA
52. W. P. Ellis, Standards Consultant, Harleysville, PA
53. P. W. Fairey III, Florida Solar Energy Center, Cape Canaveral, FL
54. W. P. Goss, University of Massachusetts, Amherst, MA
55. R. A. Grot, National Bureau of Standards, Gaithersburg, MD
56. J. L. Heldenbrand, National Bureau of Standards, Gaithersburg, MD
57. W. C. Hitchings, National Forest Products Assoc., 1619 Massachusetts Ave, N.W., Washington, DC
58. B. Howard, National Concrete Masonary Assoc., Hendron, VA
59. J. F. Kimpflen, CertainTeed Corporation, Valley Forge, PA
60. J. Klems, Lawrence Berkeley Laboratory, Berkeley, CA
61. W. M. Kroner, Rensselaer Polytechnic Institute, Troy, NY
62. S. L. Matthews, Rockwool Industries, Inc., Denver, CO
63. D. McGuire, Regal Industries, Crothersville, IN
64. K. Mentzer, MIMA, 382 Springfield Avenue, Summit, NJ
65. M. P. Modera, Lawrence Berkeley Laboratory, Berkeley, CA
66. P. G. Mulroney, VVKR, Inc., Alexandria, VA
67. R. Orlandi, W. R. Grace & Company, Cambridge, MA

EXTERNAL DISTRIBUTION (cont.)

68. B. Pierman, Dept. of Energy, Forrestal Bldg., GF-253, Washington, DC
69. W. J. Rossiter, National Bureau of Standards, Gaithersburg, MD
70. M. W. Rupp, DSET Laboratories, Inc., Phoenix, AZ
71. S. Selkowitz, Lawrence Berkeley Laboratory, Berkeley, CA
72. M. Sherman, Jim Walter Corporation, St. Petersburg, FL
73. P. H. Shipp, Owens-Corning Fiberglas Corp., Granville, OH
74. C. J. Shirtliffe, Bldg., R-105, UFFI Unit, National Research Council of Canada, Ottawa, Ontario, Canada K1A OR6
75. S. E. Smith, Dynatech R/D Co., Cambridge, MA
76. M. K. Snyder, Butler Mfg., Co. Research Center, Grandview, MO
77. L. G. Spielvogel, Wyncote House, Wyncote, PA
78. R. Sterling, University of Minnesota, Minneapolis, MN
79. T. W. Tong, University of Kentucky, Lexington, KY
80. R. P. Tye, Dynatech R/D, Cambridge, MA
81. M. G. Van Geem. Portland Cement Association, Skokie, IL
82. C. R. Vander Linden, Manville Corporation, Denver, CO
83. J. R. Warner, ACEC Research & Management Foundation, Washington, DC
84. Office of Assistant Manager, Energy Research and Development, DOE-ORO, Oak Ridge, TN

85-114. Office of Scientific and Technical Information, P. O. Box 62, Oak Ridge, TN